

APPLYING HOLOGRAPHIC PARTICLE IMAGE
VELOCIMETRY TO SPRAYS

By

KHUSHWANT SAINI

Bachelor of Engineering in Mechanical Engineering

Rajiv Gandhi Technical University,

Bhopal, M.P., INDIA

2008

Submitted to the Faculty of the
Graduate College of the
Oklahoma State University
in partial fulfillment of
the requirements for
the Degree of
MASTER OF SCIENCE
December, 2010

APPLYING HOLOGRAPHIC PARTICLE IMAGE
VELOCIMETRY TO SPRAYS

Thesis Approved:

Dr. Khaled A Sallam

Thesis Adviser

Dr. David G. Lilley

Dr. Frank W. Chambers

Dr. Mark E. Payton

Dean of the Graduate College

ACKNOWLEDGMENTS

I would take this opportunity to express my gratitude and appreciation to everyone involved in successful completion of my thesis.

I am very thankful to my advisor, Dr. Khaled Sallam for his valuable guidance and support. His advice and encouragement helped me to carry out this work to its present form.

I would also like to thank my committee members Dr. Frank Chambers and Dr. David Lilley for their valuable time and suggestions in improving my thesis.

The support of OKLAHOMA NASA SPACE GRANT CONSORTIUM/NASA EPSCoR through a Research Initiation Grant (RIG) in the summer of 2009 is gratefully acknowledged. The initial development of the experimental methods was carried out under the Air Force Summer Faculty Fellowship Program at the Air Force Research Lab, Wright-Patterson Air Force Base.

Last but not least, I want to thank my family and all my friends for their endless love and support.

ABSTRACT

Measuring the velocity field of dispersed flows is of major importance in many applications, such as sprays and particle-laden jets. Traditional particle image velocimetry (PIV) setup is common in laboratories but it is limited to planar measurements. The objective of the present study was to conduct velocity measurements for sprays using HPIV. The present study involved extension of present holographic PIV method to spray fields. The present optical setup is based on inline digital holographic microscopy. Double-pulsed holograms were recorded and reconstructed to yield many two-dimensional slices (planes) of the flow field at two time instances. A large number of focused and unfocused drops appeared in each slice resulting in a lot of noise. Thus it was required to develop new image processing subroutines which could bypass the noise and consider only the focused droplets present in each plane while rejecting the shadow of non focused droplets not present in plane. Threshold subroutines help user to decide the signal to noise ratio in final processed images from hologram. The PIV correlation was used to calculate velocity from images processed with subroutines.

TABLE OF CONTENTS

Chapter	Page
I. INTRODUCTION	1
1.1 General statement of the problem	1
1.1.1 Background	1
1.1.2 Problem statement	2
1.2 Previous related studies	3
1.3 Specific objectives	5
1.4 Organization of thesis	5
II. NUMERICAL METHODS	8
2.1 Introduction	8
2.2 Optical Setup and test conditions	8
2.3 Hologram and wavefront reconstruction	9
2.4 Cross correlation	10
2.5 Image enhancement	11
2.6 Particle Image Velocimetry validation	12
III. RESULTS AND DISCUSSION	22
3.1 Introduction	22
3.2 Image processing	23
3.3 Velocity vectors calculation	26

IV. SUMMARY AND CONCLUSIONS	44
4.1 Summary	44
4.2 Conclusion	45
4.3 Future Work	45
REFERENCES	47
APPENDIX A	51
APPENDIX B	59

LIST OF FIGURES

Figure	Page
1.1 Turbulent velocity measurements	6
1.2 A dual exposure hologram (Trolinger et al., 1968)	7
1.3 Shear stress measurements for hairpin (Sheng et al., 2000)	7
2.1 Setup for digital holographic microscopy (Lee et al., 2009)	14
2.2 Digital hologram reconstructed at a distance d from original plane (William 2006).....	14
2.3 Hologram of droplets	15
2.4 Reconstructed image of droplets from hologram.....	15
2.5 (a) First PIV image of wake vortex behind a model airplane (Stanislas et al., 2003).....	16
2.5 (b) Second PIV image with vortex moving Anticlockwise. (Stanislas et al., 2003).....	16
2.6 Velocity results from MATPIV	17
2.7 (a) First PIV image of axisymmetric turbulent jet	18
2.7 (b) Second PIV image of jet with particles moving towards right (Westerweel et al., 2005)	18
2.8 (a) Instantaneous velocity field (Westerweel et al., 2005).....	19
2.8 (b) Instantaneous velocity field from MATPIV.....	19
2.9 (a) Mean velocity profile (Westerweel et al., 2005)	20
2.9 (a) Mean velocity profile from PIV	20

2.10	Comparison of axisymmetric jet profile	21
3.1.	Original reconstructed slice	28
3.2.	A master slice obtained by adding multiple slices.....	28
3.3.	A filtered master slice.	29
3.4.	An outline of enhancement process for reconstructed slices	30
3.5	(a) A cropped version of master slice before filtering with blurred particles. .	31
3.5	(b) A cropped version of master slice after filtering with dark focused particles.	31
3.6	(a) Histogram of master slice two peaks containing focused and non-focused particles.	32
3.6	(b) Histogram of master slice after filter with single peak consisting of only focused particles.....	32
3.7	(a). A filtered master slice.....	33
3.7	(b). Histogram of the master slice.....	33
3.7	(c). The final thresholded image	34
3.8	(a). A master slice.	35
3.8	(b). Histogram of the master slice.....	35
3.9	(a) The filtered images using a threshold level of 50.....	36
3.9	(b) The filtered images using a threshold level of 60	36
3.9	(c) The filtered images using a threshold level of 70.....	37
3.9	(d) The filtered images using a threshold level of 80	37
3.9	(e) The filtered images using a threshold level of 90.....	38
3.9	(f) The filtered images using a threshold level of 95	38
3.9	(g) The filtered images using a threshold level of 100	39
3.9	(h) The filtered images using a threshold level of 110	39
3.9	(i). the number of focused and non focused droplets as function of the threshold value	40

3.10 (a). The number of flagged sub-windows vs. the image (pixel) intensity for different sub-windows sizes.....	42
3.11. Calculated velocity vectors using PIV algorithm	43

CHAPTER I

INTRODUCTION

1.1 General statement of the problem

1.1.1 Background

With the introduction of Particle Image Velocimetry plane measurements of whole velocity fields were made possible. Holographic Particle Image Velocimetry is derived from Particle Image Velocimetry. Holography is a tool to record three dimensional images. Early Trolinger et al. (1968) used holography to measure the dynamic properties of particles by recording double exposure holograms of aerosol sprays (Fig 1.1) but the use of holography in PIV started in the after years of 1980's. Adrian (1986) was one of the pioneers in the field of HPIV. He utilized holograms for actual correlation using PIV methods. In the early studies, HPIV holograms were recorded on photographic films which require a separate reference beam to reconstruct the image. Zhang et al.(1997) and Fabry et al.(1998) use HPIV double pulsed holograms recorded at short intervals to investigate flow fields.

After recent improvement in recording methods and the availability of cheap sensors digital holography has become a more convenient recording technique for velocimetry. Digital holograms can be easily recorded and reconstructed by using computer algorithms (Sheng et al., 2003).

1.1.2 Problem statement

In the present work the holographic PIV technique is used to study the three dimensional flow characteristics of a spray field. Holographic images of spray field are used. A large number of droplets and a lot of noise are present in these holograms due to multiple reflections. In the case of low number density dispersed particles can be easily identified but in case of dense sprays a lot of noise is present which complicates particle detection. Furthermore, when holograms are reconstructed the unfocused particles also show up in the reconstructed plane and it becomes difficult to differentiate between the particles present in the plane of reconstruction and unfocused particles which are out of plane. For an ideal PIV processing the image should only possess the particles which are travelling in the image plane. Hence, it is very useful to develop a method to remove the particles which are out of plane and remove the noise developed in the reconstructed slice. For a less dense particle field tracking algorithms can effectively identify the positions of particles but in case of a dense particle field a large number of particles are present which makes particle tracking more time consuming process. Furthermore, tracking every individual particle generates a lot of information which may not be useful for the user and at the same time this requires a lot of processing time. Most of these challenges can be met by using a particle image velocimetry routine for processing the reconstructed hologram.

1.2 Previous related studies-

The present study involves extension of present holographic PIV method to flow fields of sprays. Traditional PIV setups are limited to planar measurements. Adrian (1986) presented holograms as a potential source of imaging method for Particle Image Velocimetry. Fabry et al.(1998) used holography to do the three dimensional measurement over the flow using a forward scattering recording scheme. They combined holography and stereoscopic PIV to get orthogonal views of test volume. Reconstruction of both views gives plane of image at different depths which are correlated to get three dimensional vectors. Feldman et al.(1998) used HPIV for measuring the properties of a flash spray. Holograms were recorded from perpendicular views and reconstructed to get image at different depth, a stereo matching module was developed to determine the position of droplets and computer algorithm was employed to calculate the velocity from the information recorded on the holograms. Barnhart et al. (2000) presented a new method of processing holograms, on the basis of an image shifting technique. Holograms were reconstructed which involved less noise as compared to traditional reconstruction methods. Most of the studies till year 2000 were done on traditional holograms, they were recorded on photographic plate and required to be scanned later to get the information about the particles at desired depth. These limitations were overcome by digital holograms which can be recorded directly on CCD devices.

Digital holograms can be reconstructed on a computer using a transformation algorithm. Hinsch (2002) included digital holography in his review work and outlined the early work done in the field of digital recording and reconstruction of holograms and its use in PIV systems. Malek et al.(2004) used digital holograms for calculating three dimensional

two component velocity vectors. They used wavelet transform method to reconstruct the recorded holograms. Holograms were recorded at a short interval of time and images at different depth are reconstructed and correlated with the image from another hologram at same depth by correlating the two images vectors were obtained. Sheng et al. (2003) developed two view HPIV methods using single beam of laser. They developed a system to record the hologram by splitting the beam and recording both views on same CCD sensor. Sheng et al.(2006) developed digital holographic microscopy and showed the capability of holography to record the holograms of small particles with lesser noise due to lens-less configuration of recording. Further they employed this technique to do PIV over very small particles [Sheng et al. (2006)] and performed velocity measurements in boundary layer (Fig 1.3)[Sheng et al.(2008)]. Holography is a favorite method of researchers for three dimensional velocity measurements but in most cases holography is not used for dense flows hence individual particle tracking method is used to calculate velocity of each particle by calculating position from dual view or using multiple camera images from different directions as used by Soria and Atkinson (2008) to calculate three component-three dimensional holographic fluid measurements with a higher level of accuracy (~4.3%). Lobutova et al. (2010) also used Holographic Particle Tracking Velocimetry to calculate large scale circulations.

Most of the methods involving holography are employed for a less dense medium and involve tracking of single particle in each frame to calculate the velocity of flow. As more number of views involved more probability of calibration errors are involved in the system. Most of the research is done on single particle tracking, but these methods may not work well with dense particle region. By developing a new system based on PIV

correlation, velocity can be calculated in dense particle regions in general and sprays in particular.

1.3 Specific objectives-

The specific objectives of the present study were as follows-

1. To choose a PIV algorithm capable of doing cross correlation over slices of hologram using MATLAB and validate its performance.
2. To reconstruct holograms and do image processing to reduce the noise in the reconstructed images.
3. To develop a set of routines capable of distinguishing between the droplets and the noise present in the images and to use them for PIV to calculate the velocity field of dense sprays.

1.4 Organization of the thesis:

This thesis is organized into four main chapters. First chapter includes statement of the problem, specific objectives of present study and literature review. The second chapter describes the experimental and computational methods used for study. Results of study are presented in third chapter and finally the summary and the conclusions of the work is presented in fourth chapter.

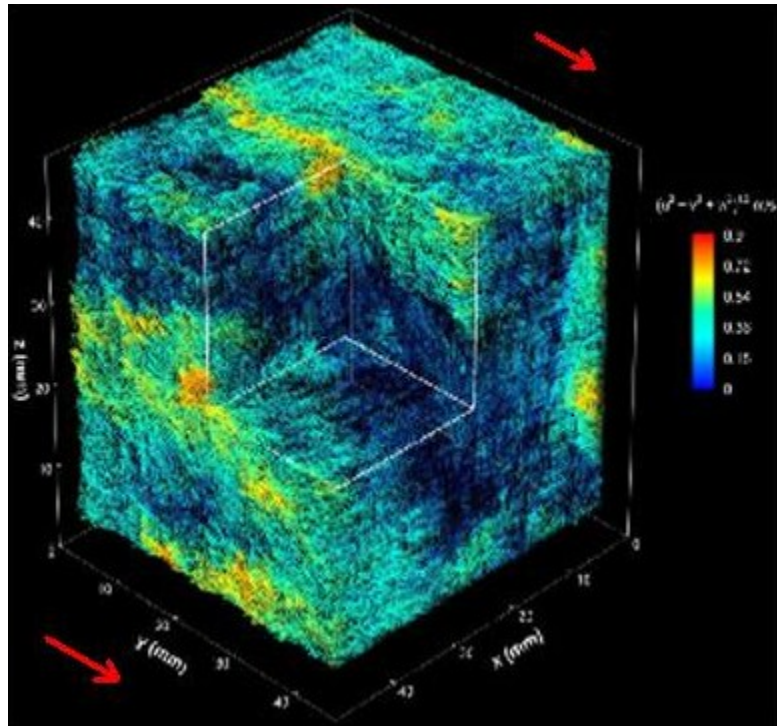


Fig1.1.Turbulent velocity measurements using HPIV

[<http://www.me.jhu.edu/%7Emeneveau/gallery.html>]

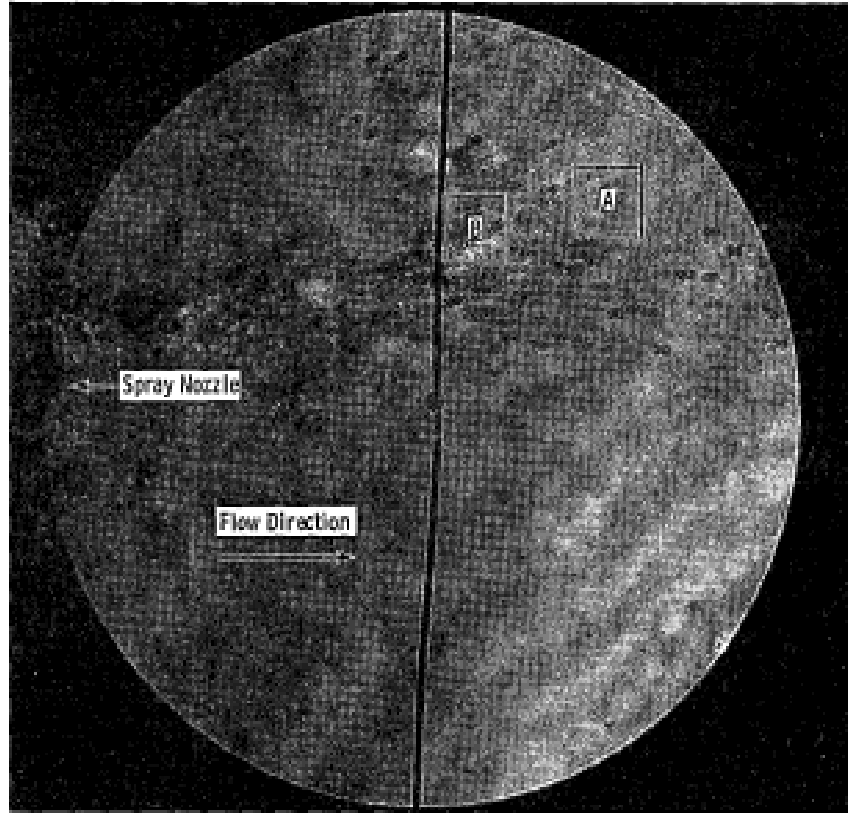


Fig 1.2. A dual exposure hologram of aerosol spray [Trolinger et al.(1968)]

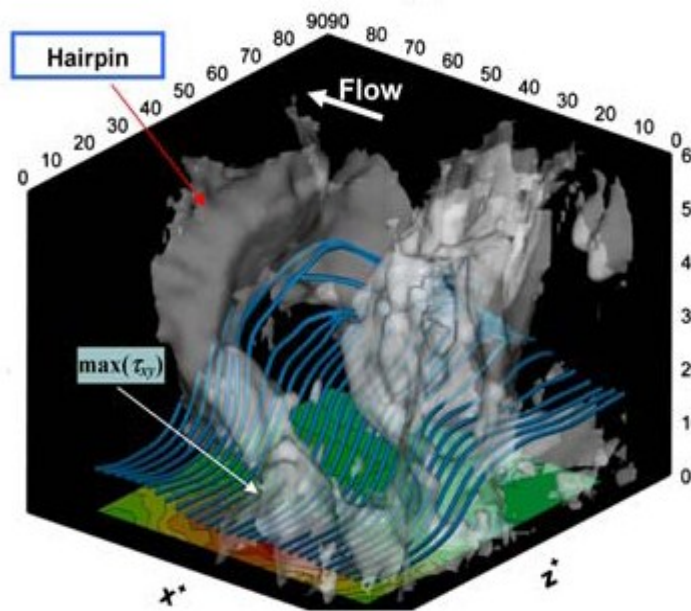


Fig 1.3. Shear stress measurements for a Hairpin[Sheng et al.(2000)]

CHAPTER II

NUMERICAL METHODS

2.1 Introduction

This chapter presents the computational methods used. The holograms were recorded using a CCD sensor. As discussed in the previous chapter the challenge lies within the number density of particles/droplets in the field of view. For high number density the holograms record almost same level of noise as signals present in it. It was required to develop a method with which the background noise of the holograms can be removed. Also, in a hologram at a particular depth reconstructed images have shadows of particles which were not present in that plane. It was required to clean the reconstructed slides before processing them with a PIV algorithm. In the current chapter the method used for recording and the reconstructing the holograms is presented as well as the correlation algorithm used to calculate velocity.

2.2 Optical Setup and test conditions

Holograms are used to record the three dimensional volume on a 2D holographic plate or a CCD in the case of digital holograms and then reconstructed numerically. The

recorded holograms were based on an optical setup consisting of Nd:YAG laser acting as a monochromatic light source needed to illuminate the test volume. The optical setup is shown in fig 2.1. The test conditions of that experimental setup can be found at Sallam et al. (2010).

2.3 Hologram and wavefront reconstruction

Holograms are generated by interference of two coherent waves, one of the waves is shone onto the object. Another wave is used as reference wave. Both waves are made to interfere at the recording surface. In case of digital hologram the recording surface is a CCD or a CMOS camera. For in line holography a single beam is used as both an object wave and a reference wave. In this case the part of the beam which diffracts from the objects serves as object wave while the rest of the beam which remains unchanged acts as a reference wave. Both these waves interfere on the surface of camera and the information is stored as an interference pattern. The method of numerical reconstruction as explained by William et al. (2002) is as follows:

The recorded intensity is given by following the term:

$$I_H(X, Y) = (R+O)^* \cdot (R+O) = |R|^2 + |O|^2 + R^*O + RO^* \quad (1)$$

Where R is the reference wave and O is the object wave. The last two terms are cross product terms and they represent the interference of the waves in a hologram. The wavefronts are reconstructed by multiplying the recorded hologram intensity with a reference wave as follows:

$$R \cdot I_H = R \cdot (R+O)^* \cdot (R+O) = R \cdot (|R|^2 + |O|^2) + |R|^2 O + R^2 O^* \quad (2)$$

Here the first term on the right hand side represents the reconstruction of zero order terms hence they are neglected while the second term represents the virtual image which can be reconstructed by propagating over a distance d in space and the third term represents an outgoing wave which is a mirror image of the virtual image with respect to the hologram. Real image is obtained by multiplying I_H by R^* and propagating it to a distance $(-d)$ in the space which gives O^* in real image plane (Fig 2.2). In discrete form $I_H(k\Delta x, l\Delta y)$ is the hologram intensity which is superposition of object wave $O(k\Delta x, l\Delta y)$ and reference wave $R(k\Delta x, l\Delta y)$ and it is required to filter the OR^* terms from the spectrum but the objective wavefield O_H in plane of hologram is given as:

$$O_H(k\Delta x, l\Delta y) = I_H \text{ filtered}((k\Delta x, l\Delta y) R((k\Delta x, l\Delta y)/|R|^2) \quad (3)$$

Now to reconstruct the hologram a digital reference wave is artificially generated in the reconstruction algorithm which acts as normal reference beam but allows the adjustment of parameters, and it is given by following mathematical expression:

$$R_D(k\Delta x, l\Delta y) = |R_D| \exp[i(k_x.k\Delta X + k_y.l\Delta y)] \quad (4)$$

By using the above expression for the reference wave the object wave is reconstructed by propagating the recording plane $x-y$ to the target plane $\xi-\eta$ (T)

$$O_T(m \Delta \xi, n \Delta \eta) =$$

$$-I \exp (2i\pi d/\lambda) DF_{\text{fresnel}} T [I_H \text{ filtered} (k\Delta x, l\Delta y) R_D(k\Delta x, l\Delta y)/|R_D|^2] \quad (5)$$

Samples of hologram recording and reconstruction are shown in figures 2.3 & 2.4.

2.4 Cross Correlation

To calculate the velocity vectors it is necessary to process two images obtained between two time instants. The basic principle behind velocimetry is the correlation of these two images which involves matching the pattern of particles found in one image with other image. Pattern matching involves dividing the image into smaller sub-images and matching the sub-windows formed with the same window in the other image (at the second time instant). The matching process involves changing the position of sub-window in the second image so as to find the exact position which matches the pattern of the particles present in first image. To calculate the spatial shift of the particles between the two images sub-windows are chosen which are represented by $I_1^{i,j}$, where i, j represent the sub window numbers in first image. Similarly $I_2^{i,j}$ represent the numbers of sub-window in the corresponding (second) image. Equations 6 and 7 are used by Sveen (2004) to calculate the displacements of the particles between the image pair as follows:

$$R_g(s, t) = \sum_{m=0}^{M-1} \cdot \sum_{n=0}^{N-1} [I_1^{i,j}(m, n) - I_2^{i,j}(m - s, n - t)]^2 \quad (6)$$

The above expression can be simplified as:

$$R_g(s, t) = \sum_{m=0}^{M-1} \cdot \sum_{n=0}^{N-1} [I_1^{i,j}(s, t) \cdot I_2^{i,j}(m - s, n - t)] \quad (7)$$

Equation 7 represents the cross correlation of the terms between the two sub-windows which is the basis of the algorithm used to calculate the vectors from the reconstructed image pairs.

2.5 Image enhancement

Holograms are reconstructed using the Fast Fourier Transform method but due to the presence of a large number of droplets in the image it is hard for a cross correlation algorithm to detect the difference between the noise present in the image and the particle (in this chapter particles are droplets are used interchangeably) positions. The reconstructed images are filtered using the software ImageJ. The filtered images are filtered with a set of programs written in matlab.

2.6 Particle Image Velocimetry validation

For calculating the velocity vectors of the droplets within the test volume a PIV algorithm is used. This algorithm is capable of performing cross correlation over a large number of reconstructed slides generated from each hologram. The PIV software MATPIV written by J.K. Sveen (2004). This MATLAB toolbox is used to process batch files generated after processing and enhancing the 2 dimensional images. The toolbox uses two methods of matching the sub-window as (1) cross-correlation and (2) minimum quadratic difference. The cross correlation method is used in all PIV calculations to correlate the images and depending on the size of the image and the number of particles present the size of sub-windows is estimated to take into account the displacements of the particles. To validate the program, two test cases were used from the PIV challenge competition. The results and the explanations of the test setup is published by Stanislas et al. (2003).

Test case A: This set of images was used to study wake vortex behind a model aircraft in a wind tunnel. The measurement area was 170mm×140 mm. The image size was 1024

$\times 1024$ pixel. The set of images is shown in Fig 2.5. Both images were processed with MATPIV program using a sub window size of 256 pixels. The results from the program were plotted in Fig 2.6. The figure shows the change in particles positions and the formation of a wake. The lengths of these vectors represent the average velocities.

Test Case B: This set of images shows the fluid flow in an axisymmetric turbulent jet with stagnant surroundings. The images in Fig 2.7 have a size of 992×1004 pixel. These set of images were used as test images for PIV challenge in 2003 and the details of the setup are included in Westerweel et al. (2005). The velocity vectors were calculated with MATPIV using sub-windows with a size of 128 pixels. The instantaneous and mean velocity profiles are compared in Fig 2.8 and Fig 2.9. The Axisymmetric jet here is self-similar in nature, velocity profile from calculated result is compared with theoretical velocity profile from Pope (2000) in Fig 2.10.

The results from both cases show that MATPIV algorithm is effective in calculating the velocity vectors from PIV images and can be used for further calculations of velocity vectors from reconstructed (cleaned) hologram images.

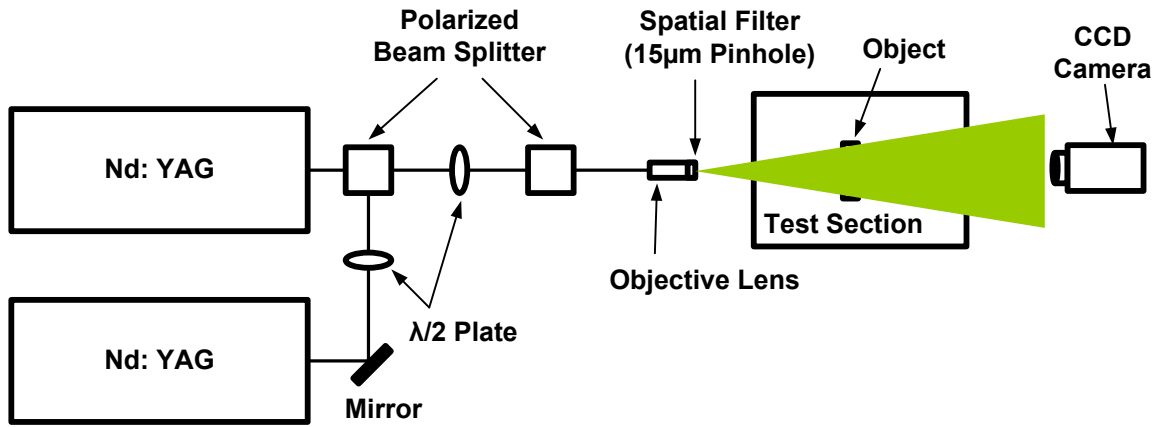


Fig 2.1 setup for digital holographic microscopy (Lee et al.(2009)).

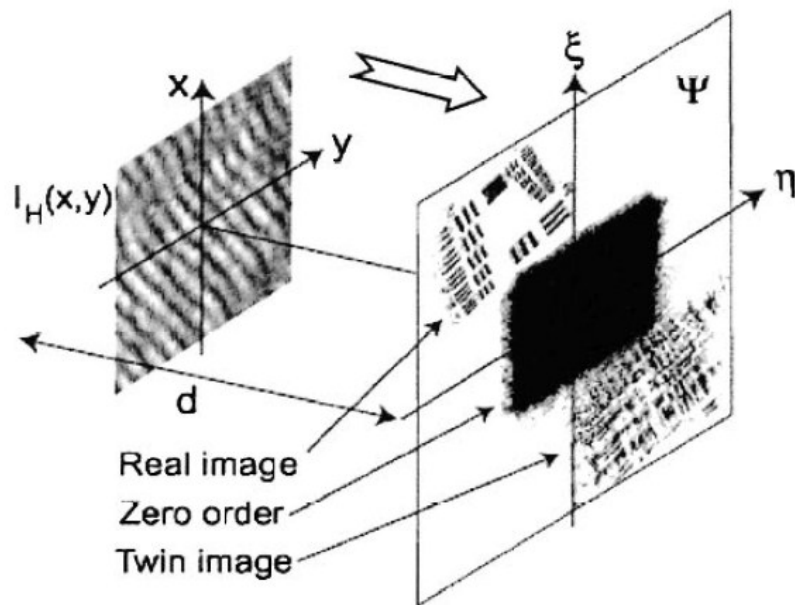


Fig 2.2. - Digital hologram reconstructed at a distance d from original plane [William, 2006].

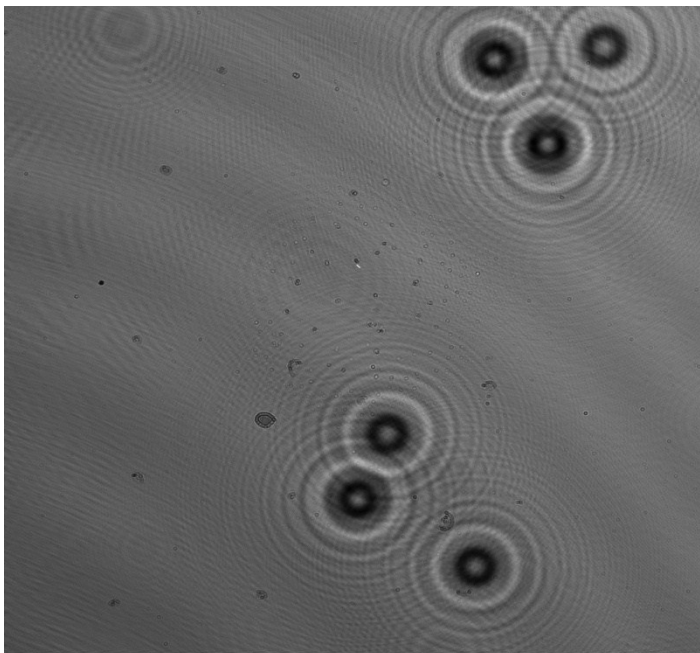


Fig 2.3- Hologram of droplets.

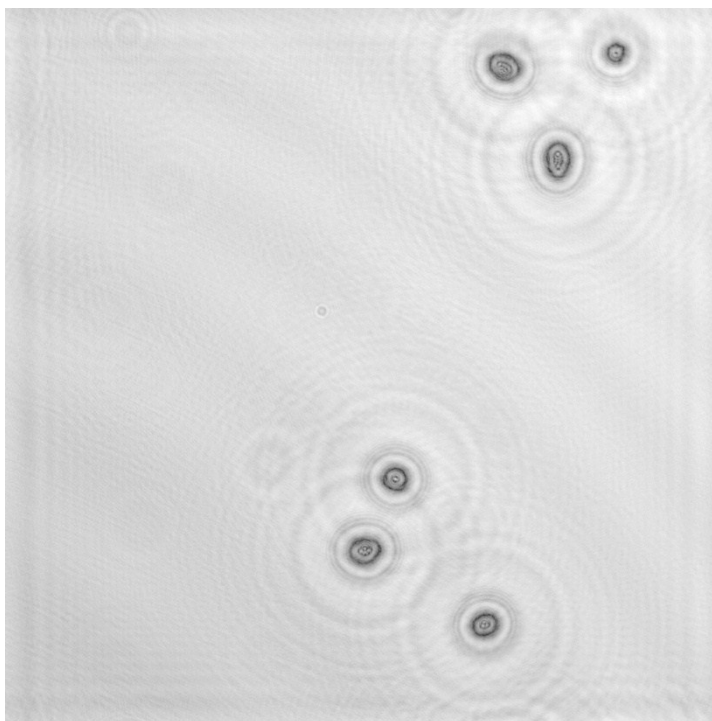
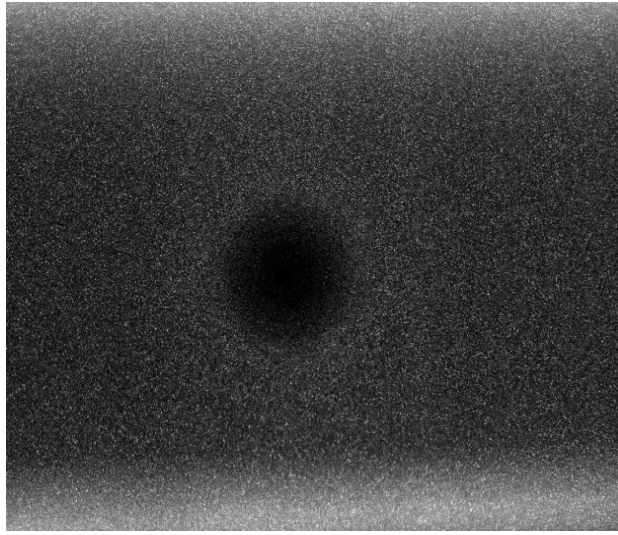
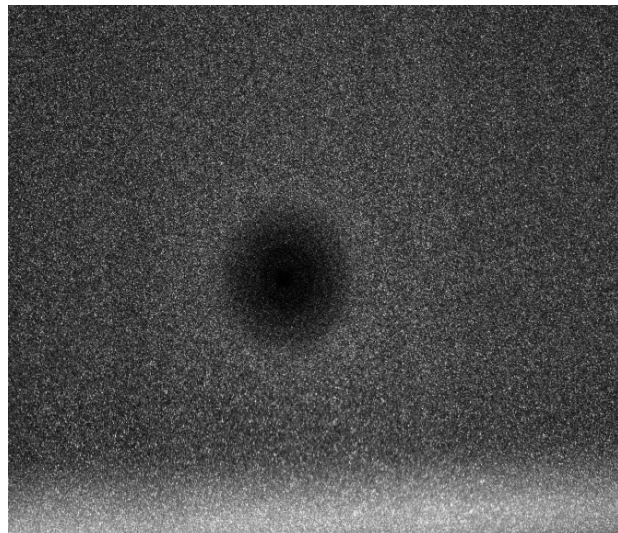


Fig 2.4- Reconstructed image of droplets from hologram.



(a)



(b)

Fig 2.5- (a) First PIV image of wake vortex behind a model airplane.
(b) Second PIV image with vortex moving anticlockwise. (Stanislas et al., 2003)

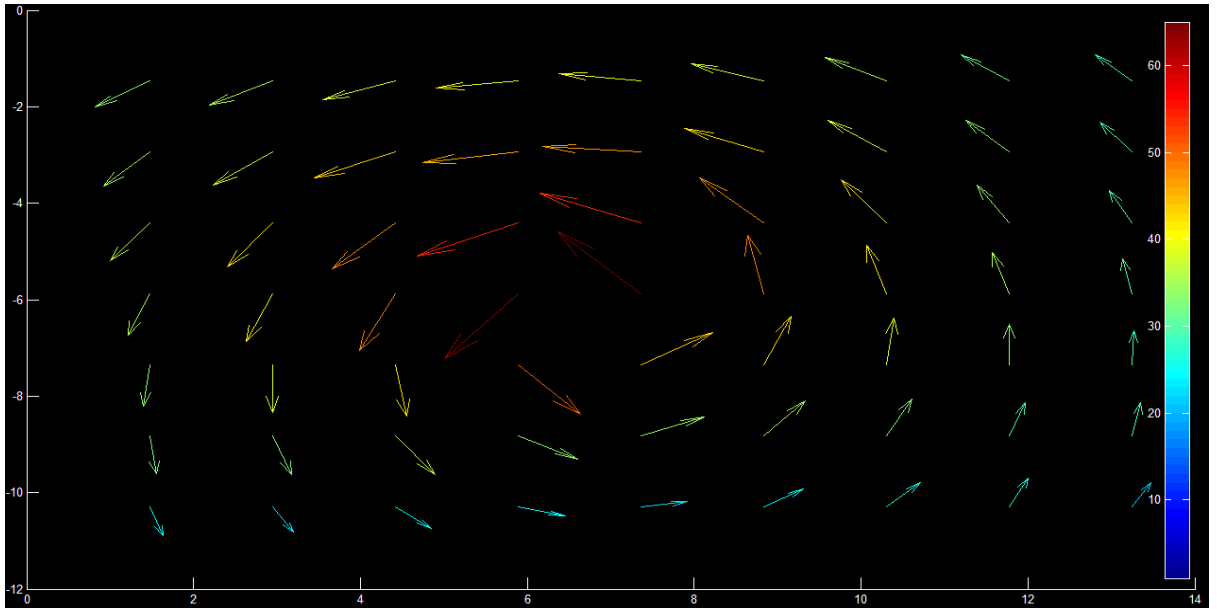


Fig 2.6- velocity results from MATPIV.

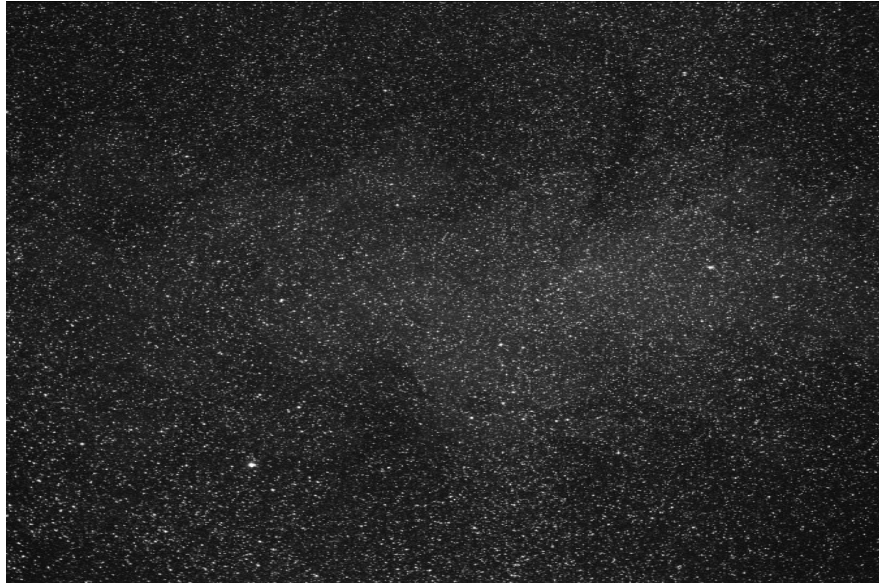


Fig 2.7 (a) First PIV image of axisymmetric turbulent jet [Westerweel et al. (2005)]



Fig 2.7(b) Second PIV image of jet with particles moving towards right [Westerweel et al. (2005)]

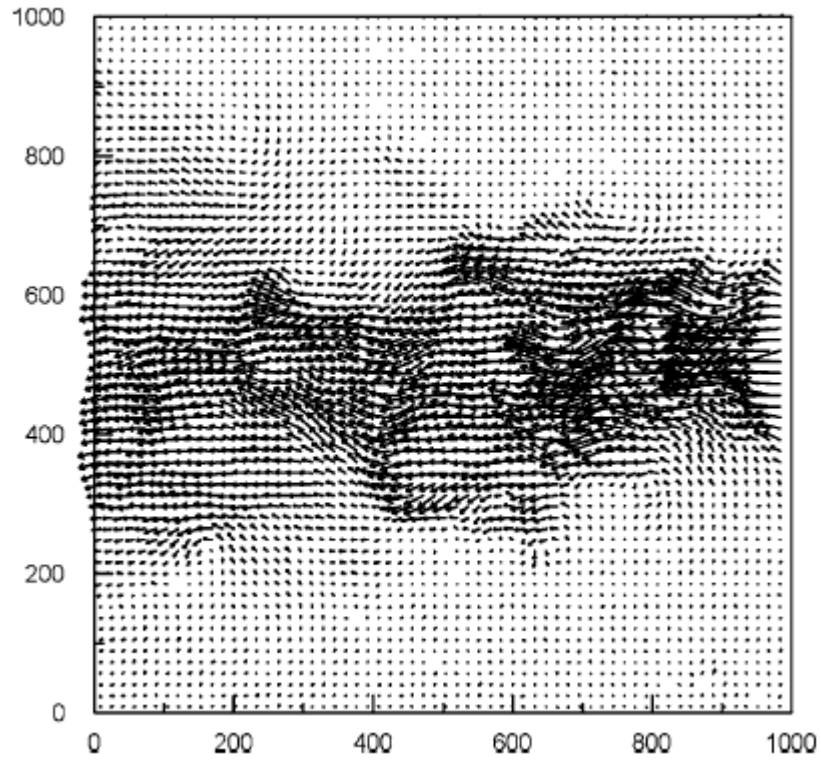


Fig 2.8 (a) Instantaneous velocity field [Westerweel et al. (2005)]

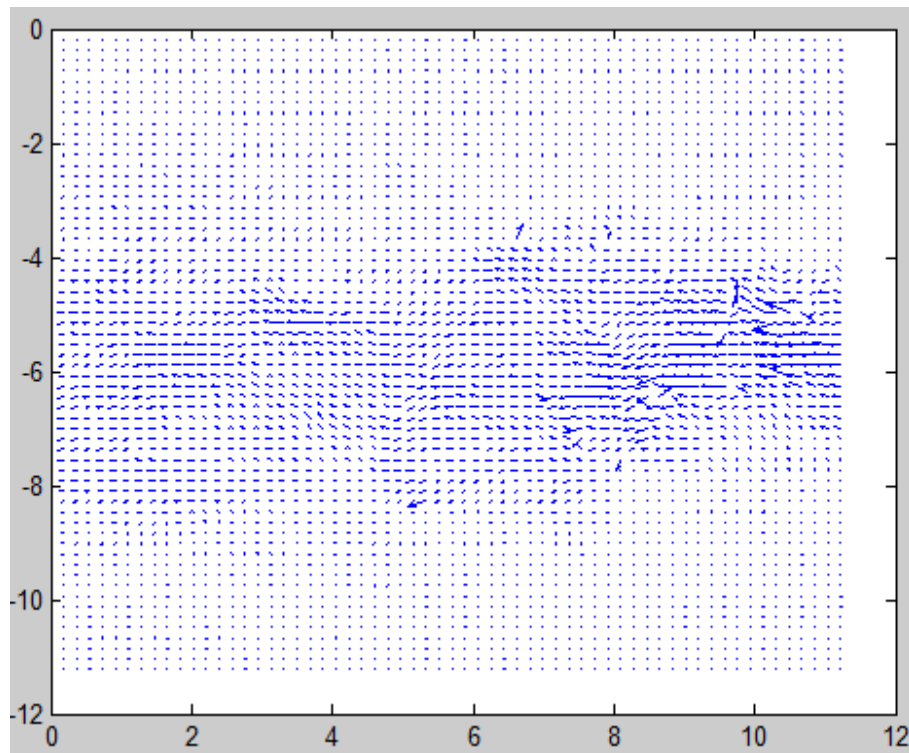


Fig 2.8 (b) Instantaneous velocity field from MATPIV

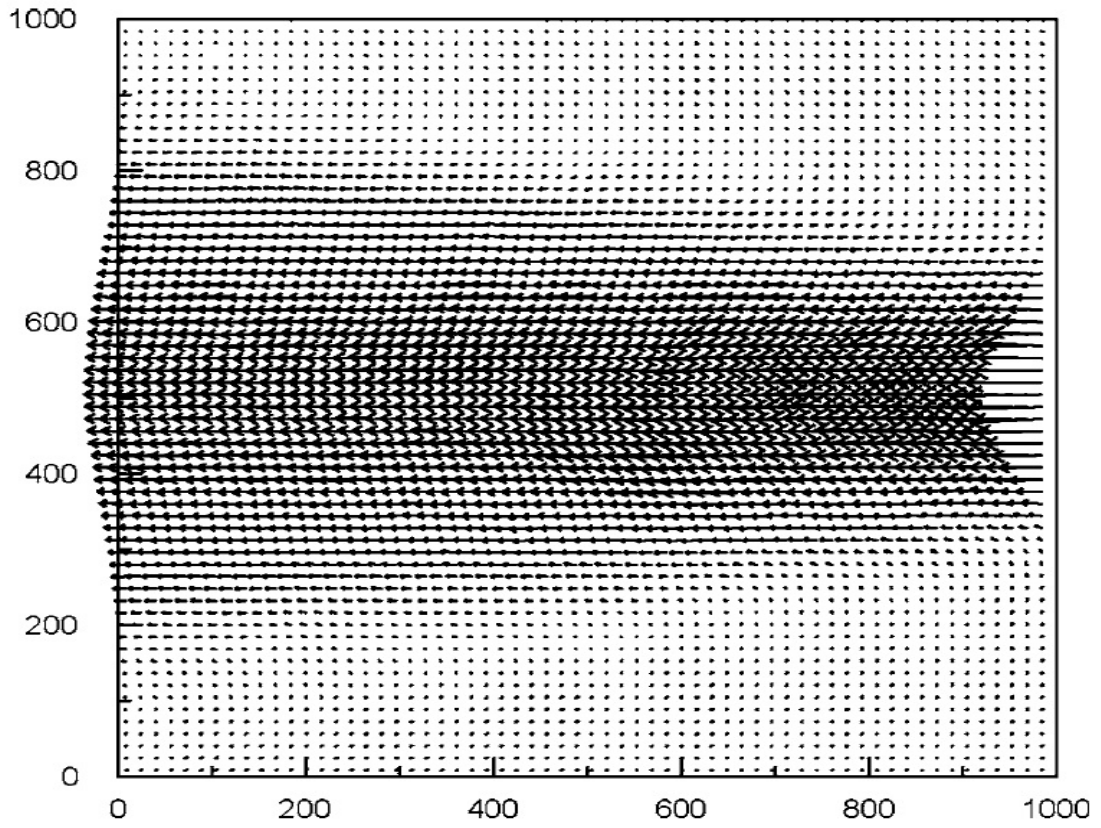


Fig 2.9 (a) Mean velocity profile [Westerweel et al.(2005)]

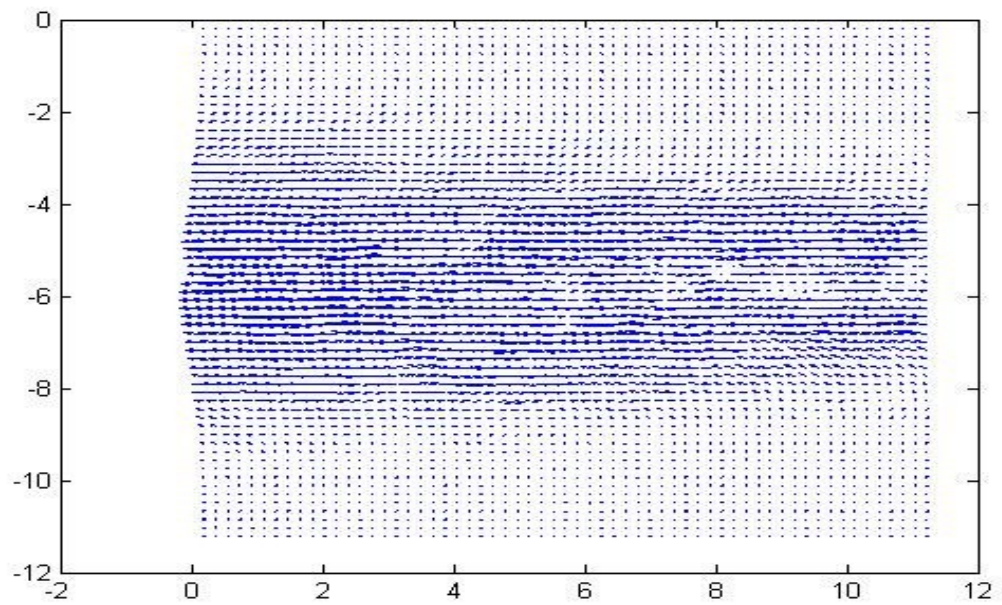


Fig 2.9 (a) Mean velocity profile [Westerweel et al.(2005)]

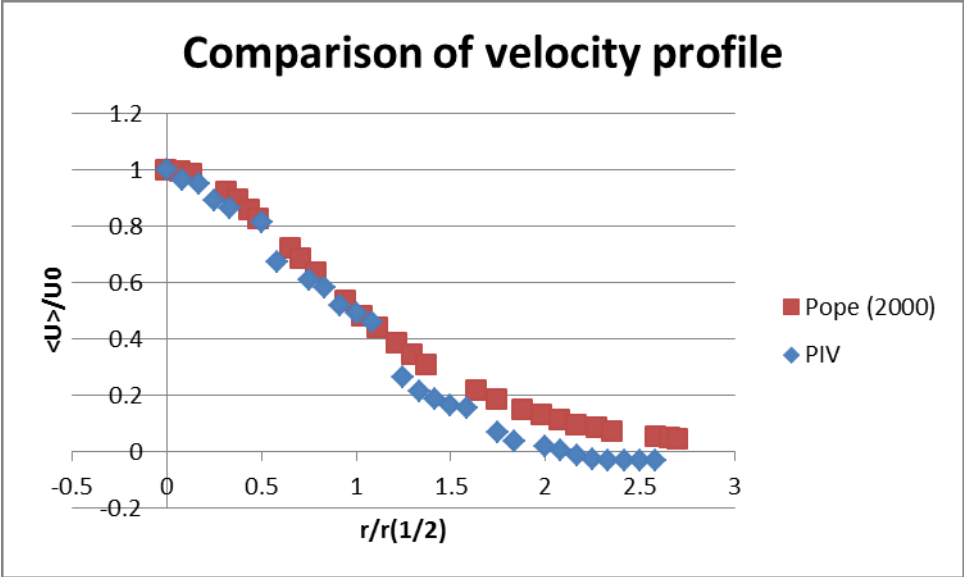


Fig 2.10 Comparison of axisymmetric jet profile

CHAPTER III

RESULTS AND DISCUSSION

3.1 Introduction

This chapter presents the image reconstruction and image processing techniques used to improve the image quality before they could be processed with PIV algorithm to calculate the velocity vectors. A numerical reconstruction program is used which gives the reconstructed slices of image at different spanwise (normal to the camera) locations within the test volume. Due to the presence of a large number of droplets it was sometimes challenging to identify the droplets which are present at a particular spanwise location. To solve this problem the reconstructed slides were processed through a subroutine written in MATLAB to reduce the noise created by out-of-focus droplets within these slides. A filtering program based on a specified threshold level was developed to remove the images of out-of-focus droplets as well as other noise sources within the images to improve the signal to noise ratio. The program is based on the difference in the pixel values of the focused droplets present in the image plane and the pixel values of the other noise sources. Finally a procedure is presented to help the user in deciding the threshold level.

3.2 Image processing

A Hologram is interference pattern recorded to store the three-dimensional visual information of the test volume. In present test conditions many factors affect the quality of the recorded holograms and the reconstruction of the information stored in them. A large number of droplets could be present in the test volume which increases the noise in the reconstructed holograms. The reconstruction of the hologram in the present study results in multiple sliced two-dimensional images. Those two dimensional images would typically have many focused droplets as well as many non-focused droplets (out of the image plane) as shown in Fig 3.1. In order to be able to apply a PIV algorithm to extract velocity information of the spray field successfully, the image should ideally include only the particles which are physically present within the image plane whereas all other out-of-focused droplets and other noise should be eliminated. Therefore, it is necessary to process the slides before feeding them to a PIV algorithm. It is desired to increase the contrast ratio of the image and to make the particles clearly visible compared to the background. To increase the difference in contrast between the focused and non focused droplets multiple slices were added to form what would be called a “mater slice” in the present study. Due to that addition, the pixel values of non focused droplets decreased and the pixel values of focused particles increased. A MATLAB routine was used to add the slices. The whole image was divided by the number of slices.

$$N'=N/ (n) \tag{1}$$

Where N is the original pixel value for image and n is the number of slices added to make the master slice.

In the present study 40 slices were added to make one master slice. Figure 3.2 shows the master slice which contain a better contrast ratio and less noise compared to any of the original reconstructed slices. The drawback of this summation is of course the loss of spatial resolution in the spanwise direction; the master slice still contains information of the particle locations within the plane parallel to the camera but no record of their relative spanwise locations. Moreover, the problem of non focused droplets is still present in this newly created master slice. So one still needs to differentiate between the focused and the non focused droplets within the master slice as well as to distinguish the droplets from background noise. One solution was to use an “unsharp filter” to increase the contrast of the droplets. The software Imagej was used to filter the master slice. The unsharp filter is similar to the high pass filtering of images which in turn is based on the use of the frequency domain to apply transformation of images. The unsharp filter deblurs the image and multiplies the blurred image with the original image. The weight is the intensity of the blurred image multiplied by the original image. This multiplied image is subtracted from the original image. The result of this process is an image similar to that shown in Fig 3.3, having focused droplets with clear edges which can be easily distinguished from the unfocused particles which are blurred in this case. Figure 3.4 shows an outline process of the image processing steps. Figures 3.5 and 3.6 shows the change in the droplet visibility and the effects of the filter on the histogram of the image. After running the filtering process through the image the droplets can be clearly distinguished from the background. To extract the droplets a selective thresholding operation was developed as explained next.

Through a selective thresholding the pixels above a certain threshold value are kept in the final image and the pixels whose values do not lie within threshold band are reduced. This process is different from a normal threshold process. In the present case a band of pixel values is selected which is not modified, while the other pixel values are changed. Therefore, in the final image only the pixels representing the particles would exist. To find the appropriate threshold value a number of images were tested at different values of pixel intensity thresholding limit. The image histogram was used to collect the intensity information of these images. To decide the threshold limit, histograms from a number of reconstructed images were studied. Figures 3.7 and 3.8 show two reconstructed slices at different spanwise location with their respective histograms. A thresholding limit was chosen by testing the threshold limit on a number of images.

The level of threshold for reconstructed master slices controls the number of droplets in the image. If the threshold is too tight then there will be less focused droplets in the image at all. On the other extreme the number of droplets would increase artificially by including noise sources and unfocused droplets and hence results in errors in the PIV calculations. To test the effect of the threshold level a reconstructed image with small number of droplets was chosen. The effects of the threshold value on the number of retained droplets within the final image are shown in Figs 3.9(a)-(h). At a lower value very few droplets remained in the final image whereas at a threshold value of 110 many droplets and background noise were still present in the final image. The number of focused droplets and the number of non focused droplets retained in the final image are plotted as a function of the threshold level chosen to process the final image in Fig 3.10. The graph shows that the number of focused droplets retained in the final image approach

a saturation level where non focused droplets and noise within the image keep increasing with the change in threshold value. A reasonable threshold level can then be determined by the user based on this graph. The user can generate this graph by using a sample image with small number of droplets or a cropped portion of an image with large number of droplets, in which it is easy to identify the number of focused droplets at different threshold levels.

To automate the process of deciding a thresholding level a MATLAB routine was developed. This subroutine divides the whole image into smaller sub-windows and compares the mean pixel value of each sub-window with the test threshold value. The number of sub-windows above the threshold value (flagged sub-windows) is then plotted as a function the intensity value for different sub-windows sizes. Figure 3.11(a) shows the number of the flagged sub-windows versus the pixel value. The sub-window sizes investigated were comparable to the droplet sizes within these images. In present study the average droplet size was 18 pixels. The slope of the curve representing the average droplet size approach a maximum around a pixel value of 100 as shown fig 3.11 (b). By selecting the threshold value as 100, one would expect an optimal thresholding of the images with a large number of focused droplets and less noise.

3.3 Velocity Vectors calculation

After processing the images and obtaining the final filtered and thresholded image containing only particles the PIV algorithm is applied to images. The same process of image summation, filtering and threshold is applied to reconstructed images from

holograms recorded after certain time interval. So finally we have two slices containing particle information which can be processed with PIV algorithm.

The open source MATLAB toolbox, MATPIV, was used to calculate the velocity vectors using cross correlation over the reconstructed and image-processed two-dimensional slices. This toolbox provides different programs to conduct single pass and multiple passes PIV. The input to the toolbox is a pair of slices obtained at two time instants at the same spanwise location. The subroutine mpiv.m was used to call the files needed to calculate the velocity vectors. The image processing toolbox of MATLAB was used to read the images. To calculate the velocity vectors two general methods are available – “minimum quadratic difference (MQD)” and “cross correlation.” Multi pass cross correlation was used. The velocity vectors are calculated by cross correlating image $I_1^{i,j}$ with image $I_2^{i,j}$ as follows:

$$R(s, t) = \sum_{m=0}^{M-1} \sum_{n=0}^{N-1} [I_1^{i,j}(m, n) \cdot I_2^{i,j}(m - s, n - t)] \quad (1)$$

Where i, j represents the number of sub window for matching in pair of images. The distance between the shift of mean in the sub-windows is calculated with the help of Fast Fourier Transform. After the calculation of the peak in the sub-windows the correlated results for whole image are stored within a matrix. Finally all the results are plotted using a vector plotting program. A batch routine program is used to automate the process of conducting PIV over a large number of images.

Fig 3.12 shows the plot of velocity of particles resulting form the PIV anlysis.

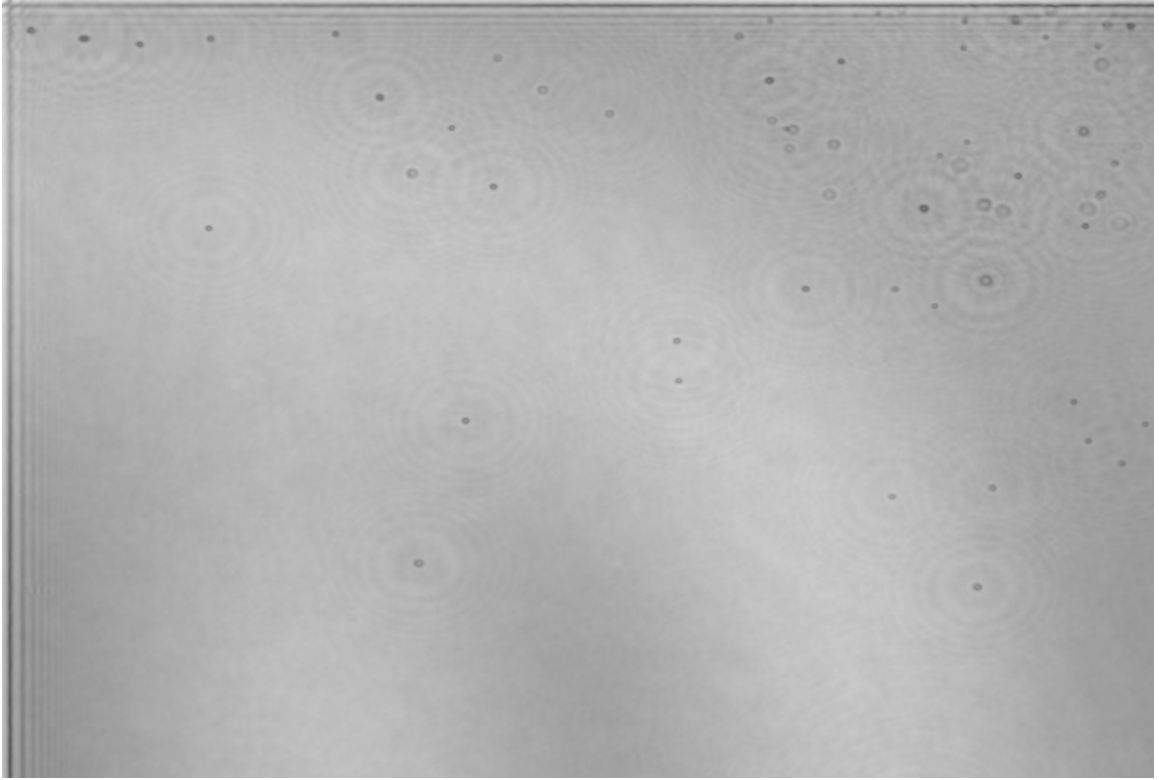


Fig 3.1. original reconstructed slice.

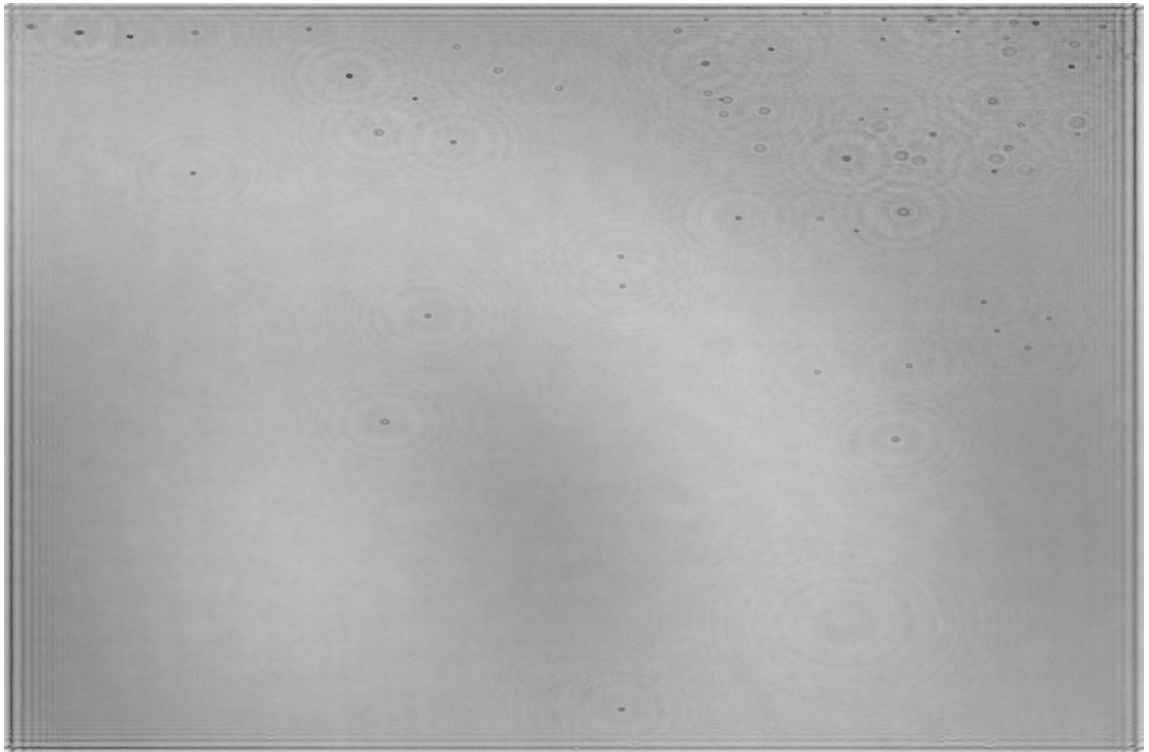


Fig 3.2. A master slice obtained by adding the multiple slices.

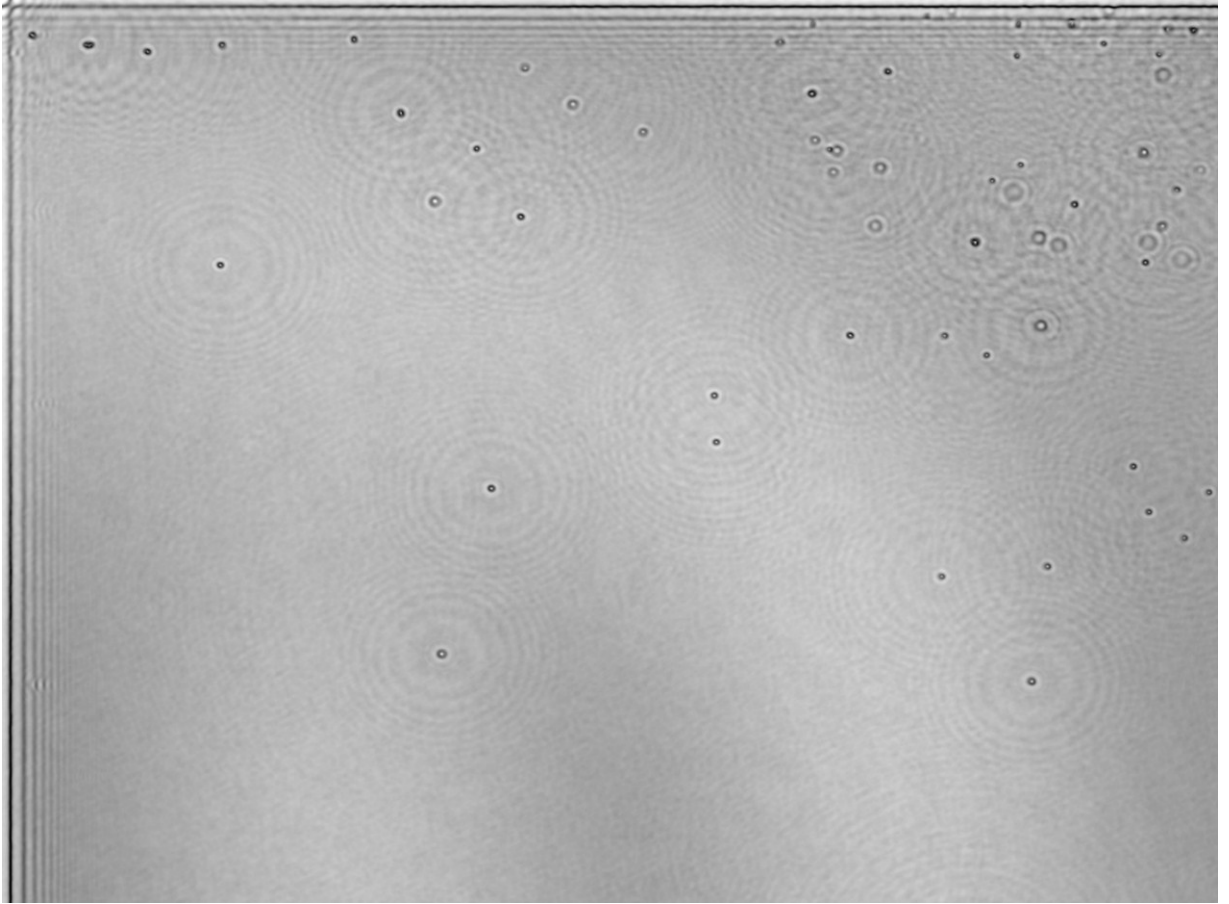


Fig 3.3. A filtered master slice.

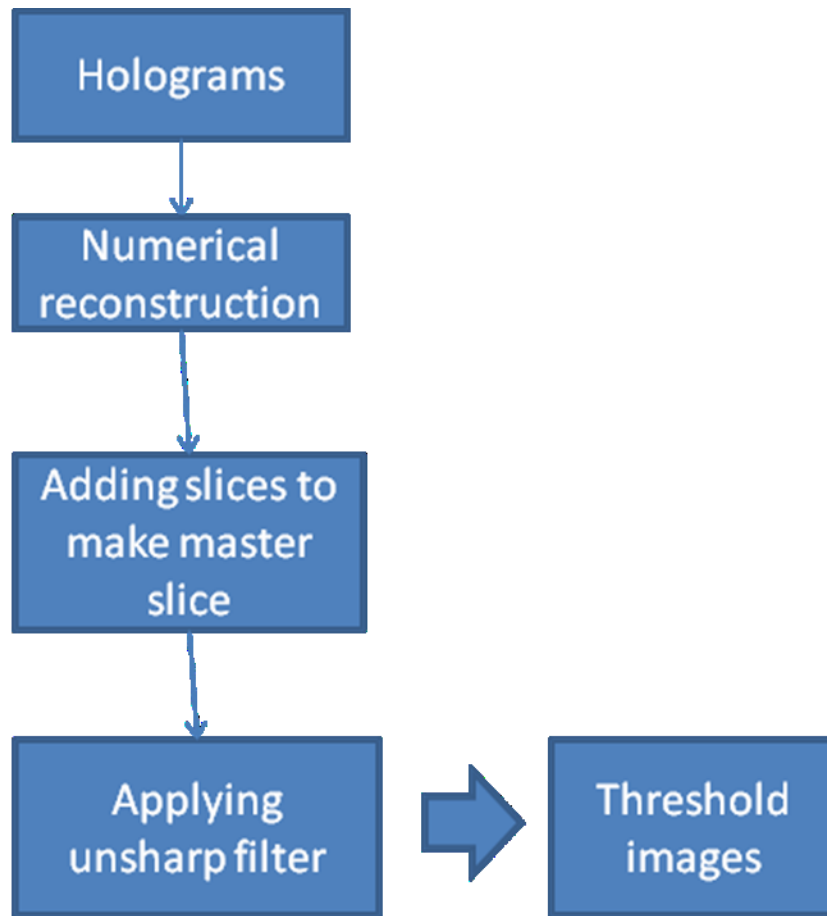


Fig 3.4. An outline of enhancement process for reconstructed slices.

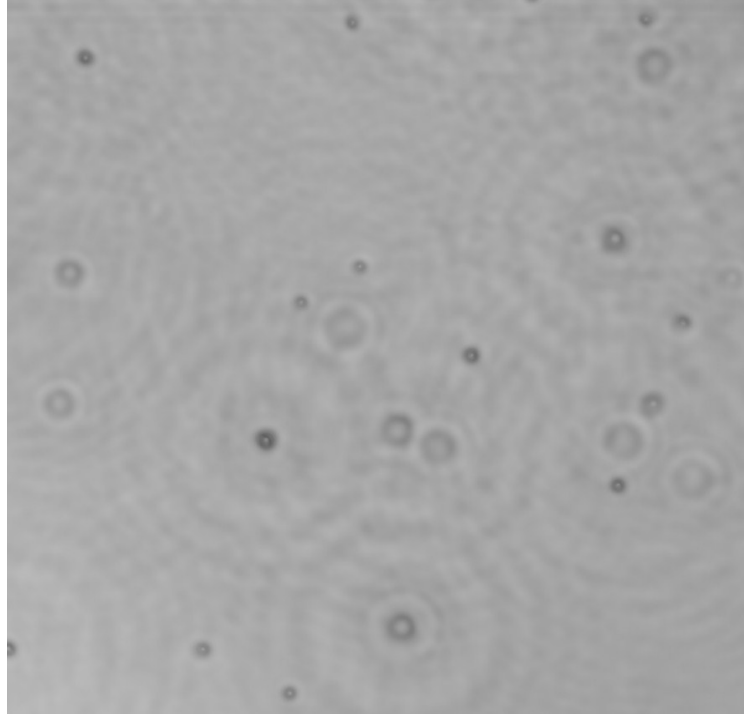


Fig 3.5. (a) A cropped version of master slice before filtering with blurred focus particles.

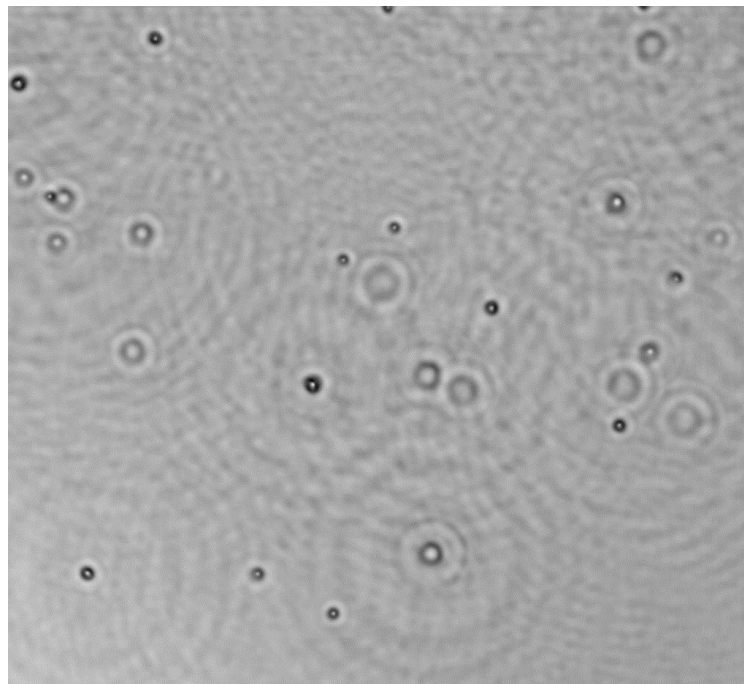


Fig 3.5. (b) Master slice with enhanced edges of focused particles after unsharp filter.

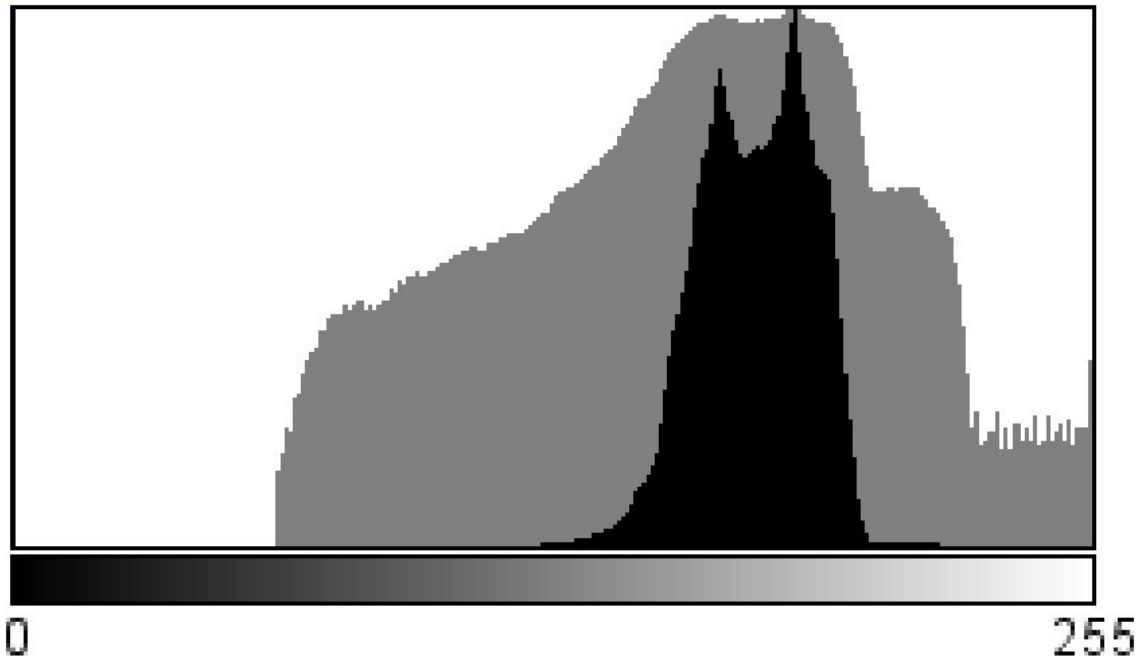


Fig 3.6 (a) Histogram of master slice two peaks containing focused and non-focused particles .

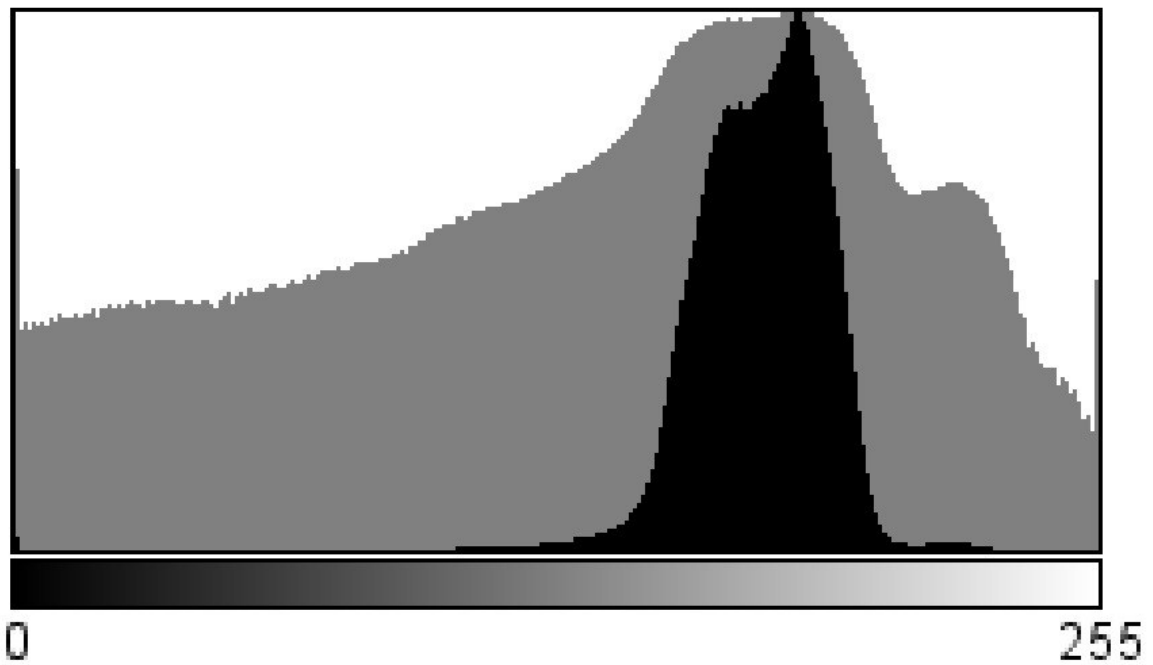


Fig 3.6.(b) Histogram of master slice after filter with single peak consisting of only focused particles

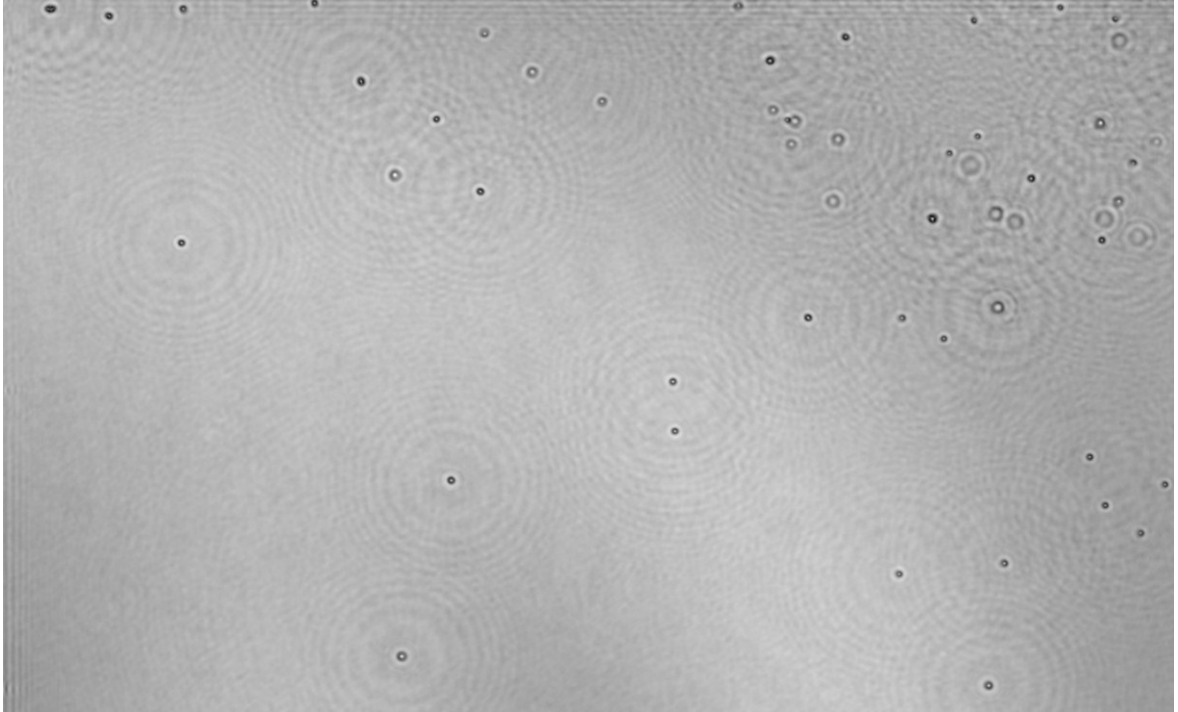


Fig 3.7(a). A filtered master slice.

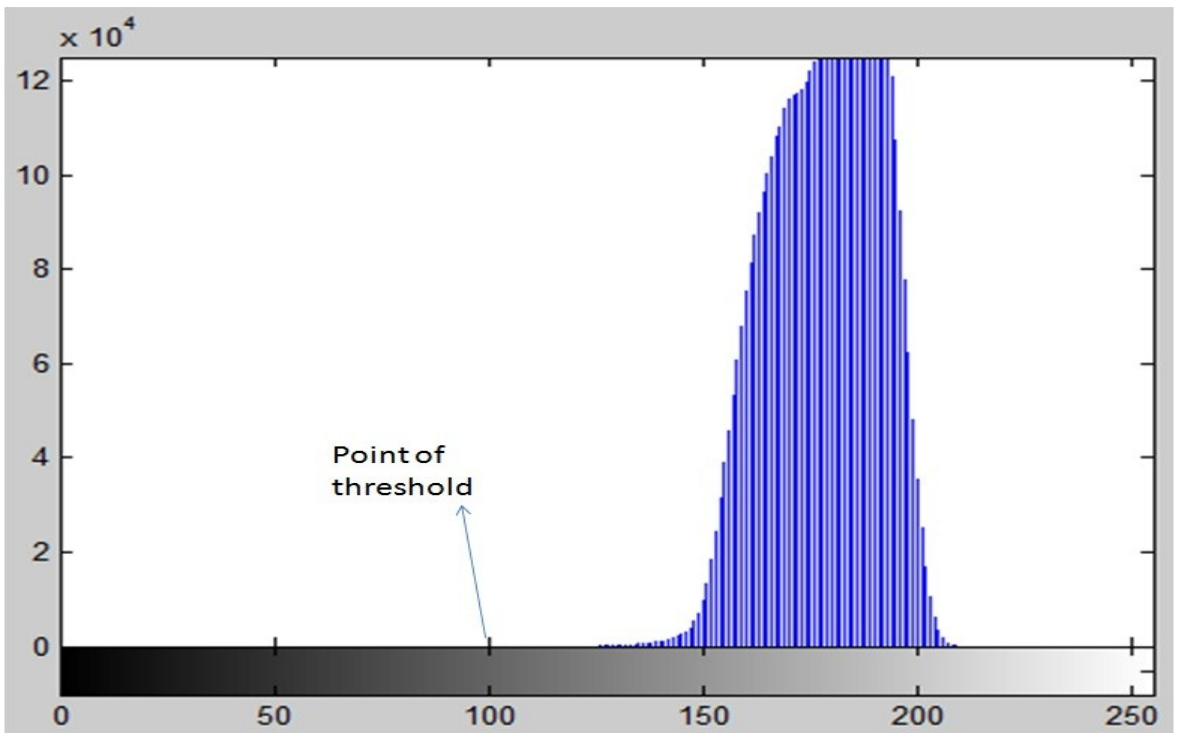


Fig 3.7(b). Histogram of the master slice.

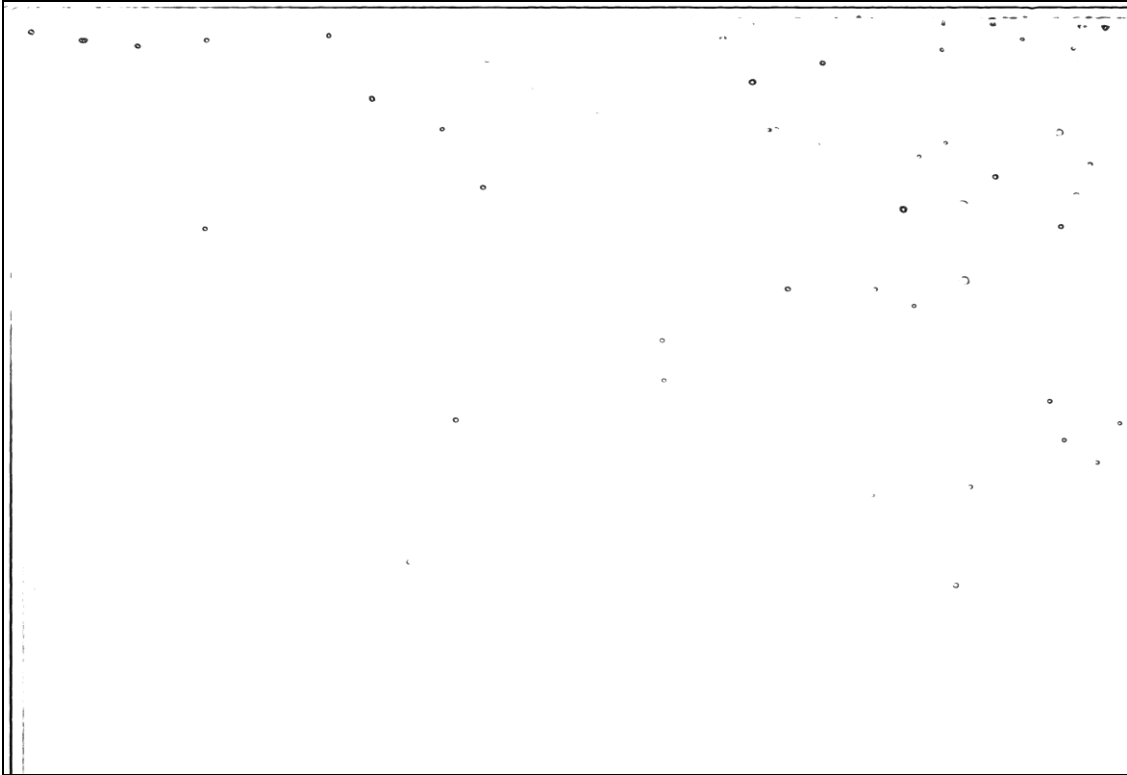
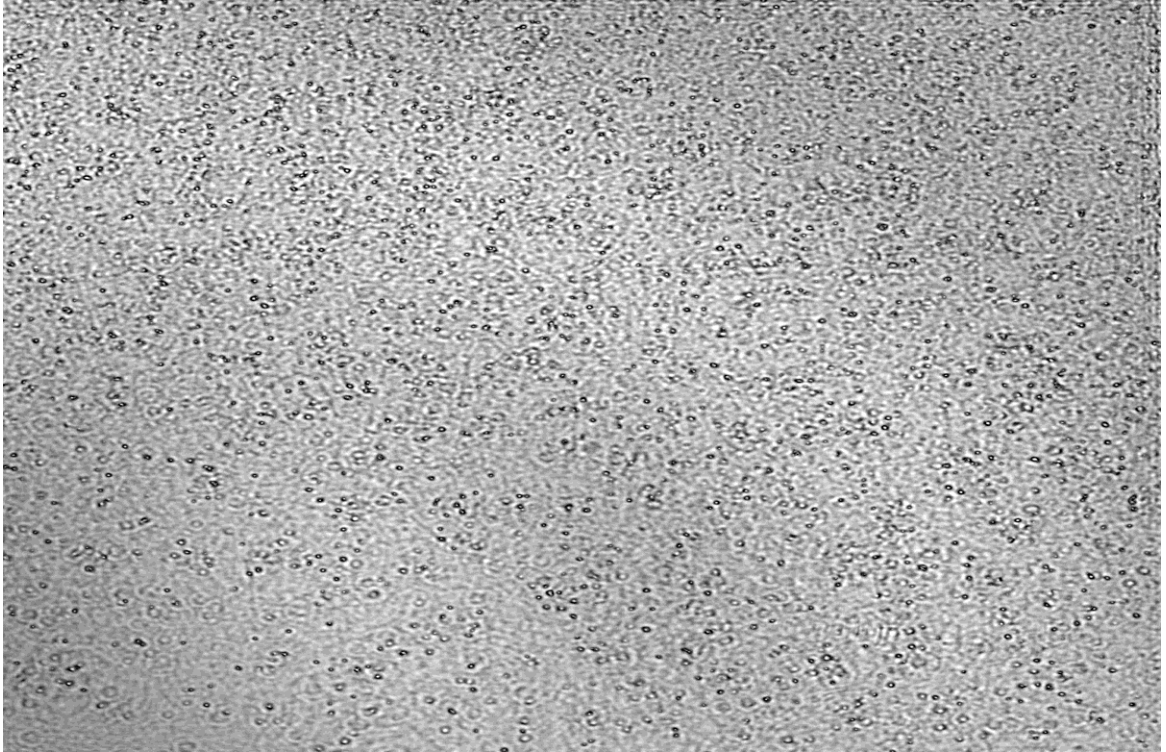


Fig 3.7(c). The final thresholded image. The filtering scheme had eliminated most of the noise and the image is mainly showing the focused particles (droplets).



(a). A master slice.

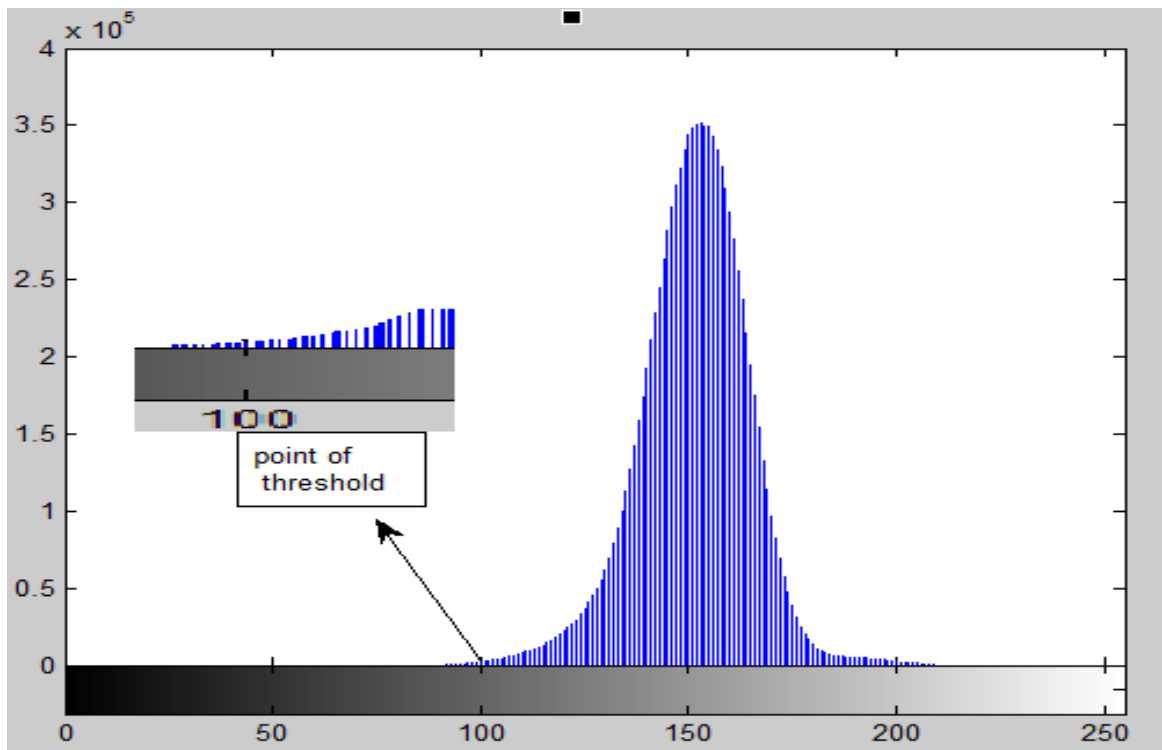


Fig 3.8(b). Histogram of the master slice.

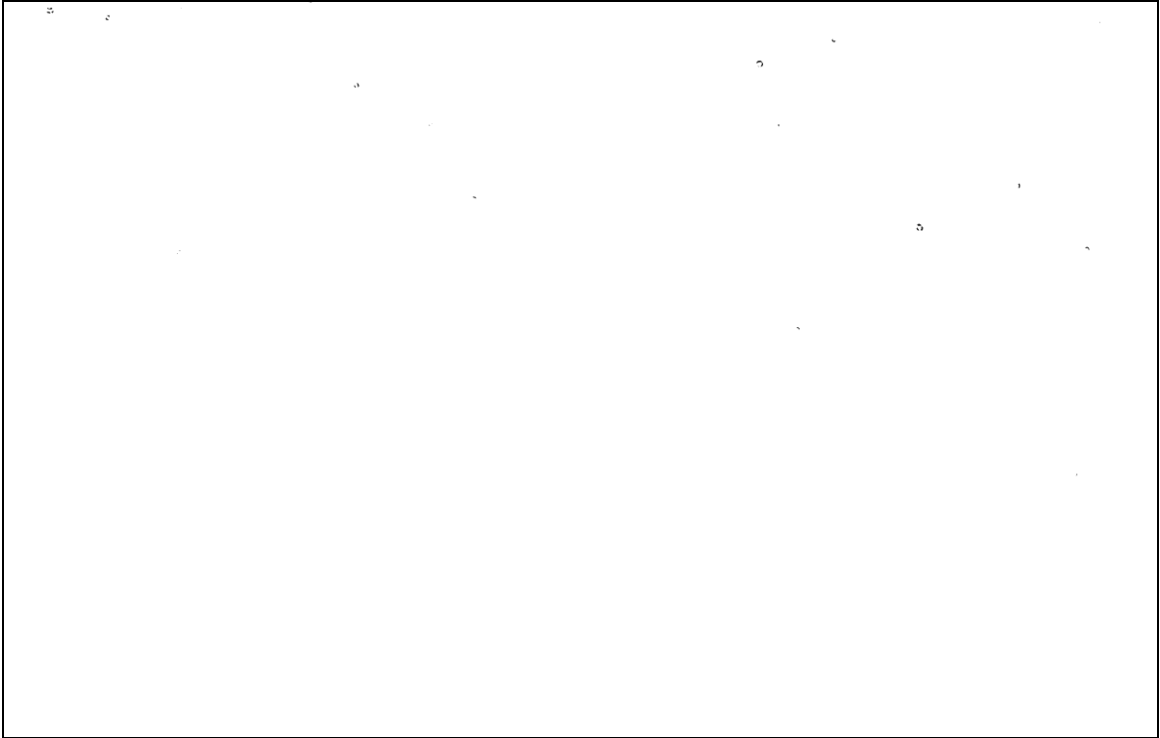


Fig 3.9(a). The filtered image using a threshold level of 50.

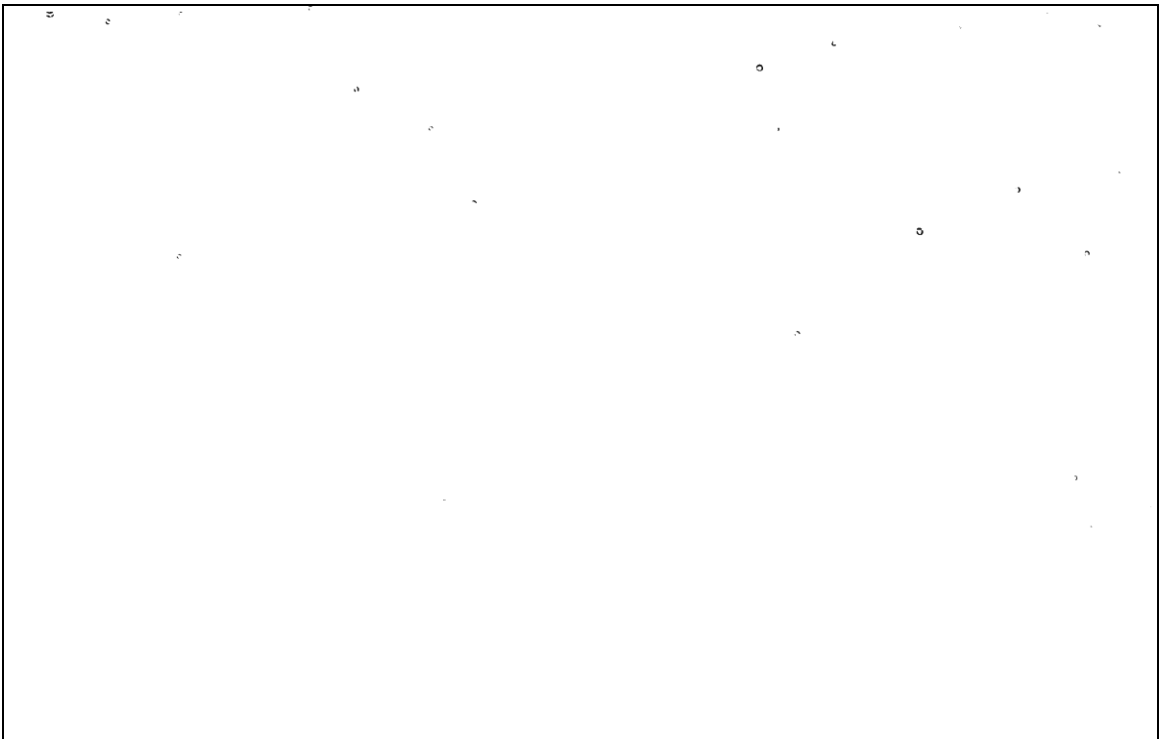


Fig 3.9 (b). The filtered image using a threshold level of 60.

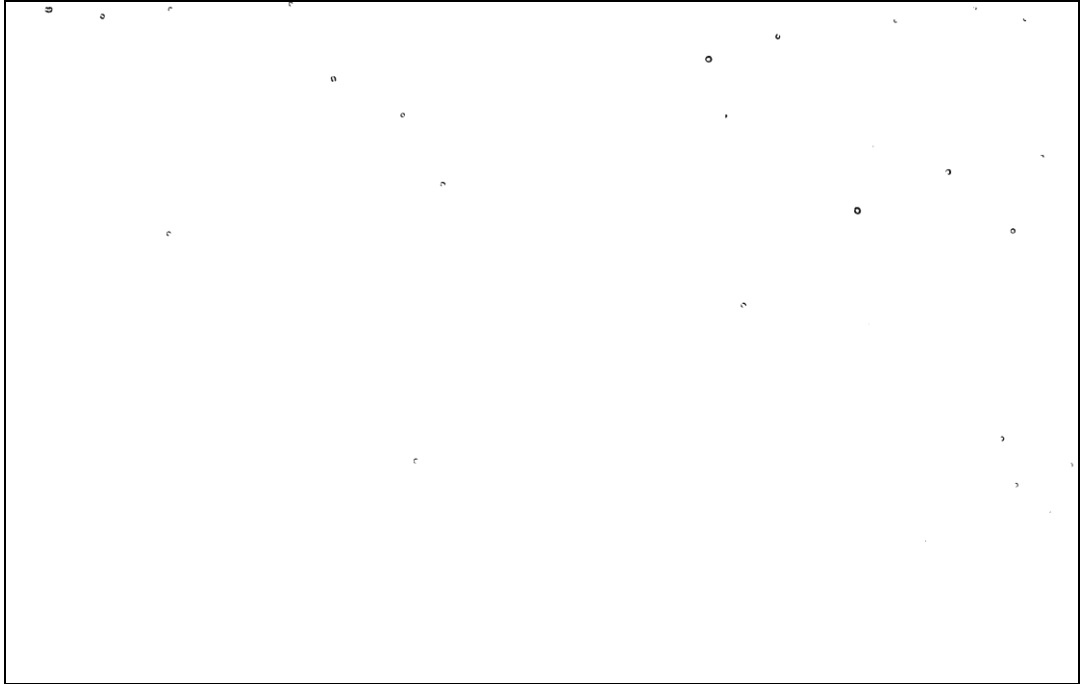


Fig 3.9(c). The filtered image using a threshold level of 70.

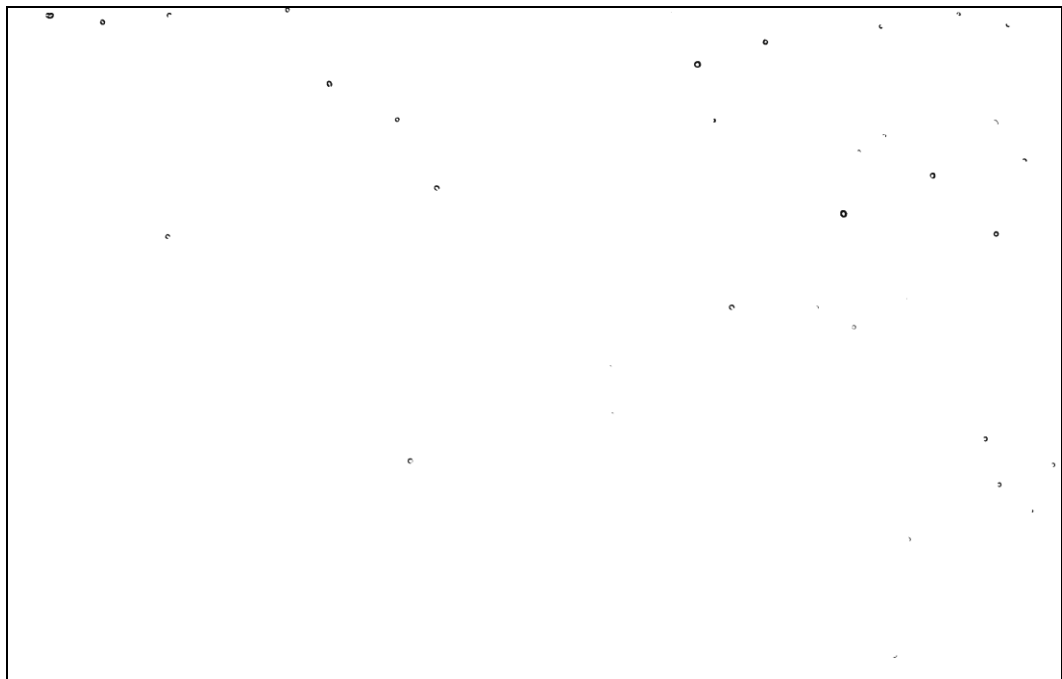


Fig 3.9(d). The filtered image using a threshold level of 80.

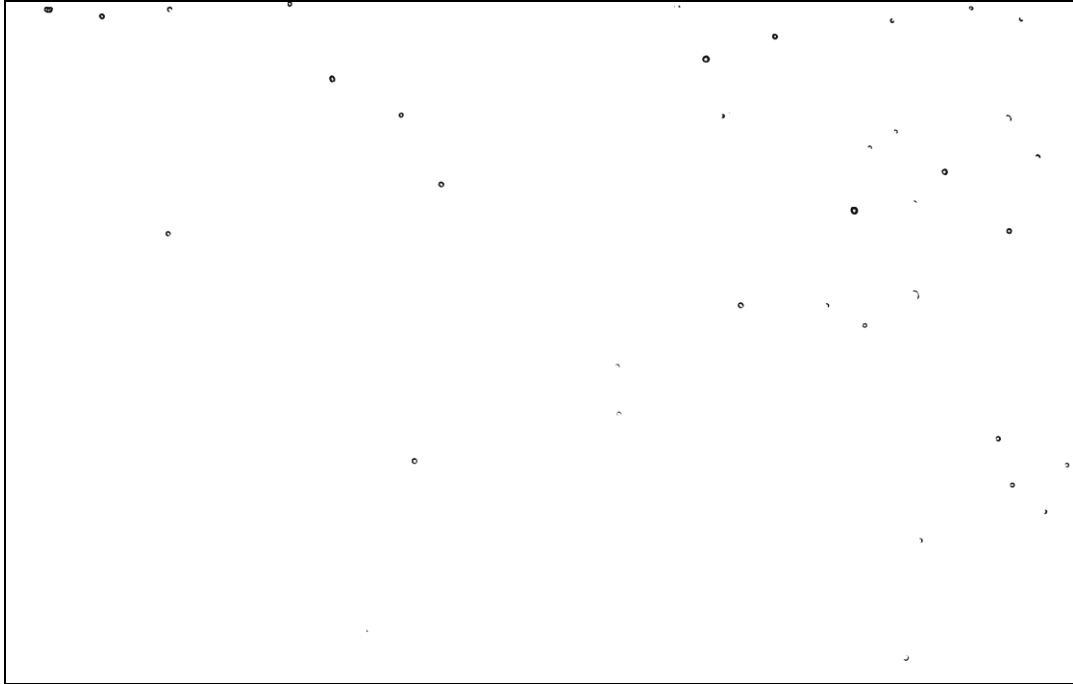


Fig 3.9(e). The filtered image using a threshold level of 90.

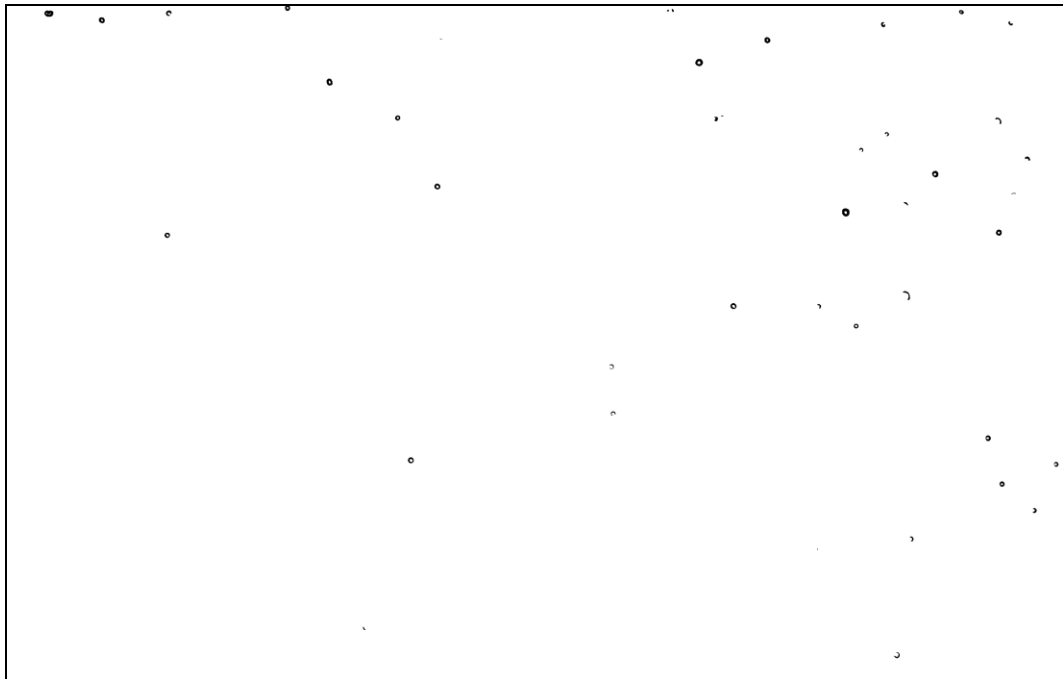


Fig 3.9(f). The filtered image using a threshold level of 95.

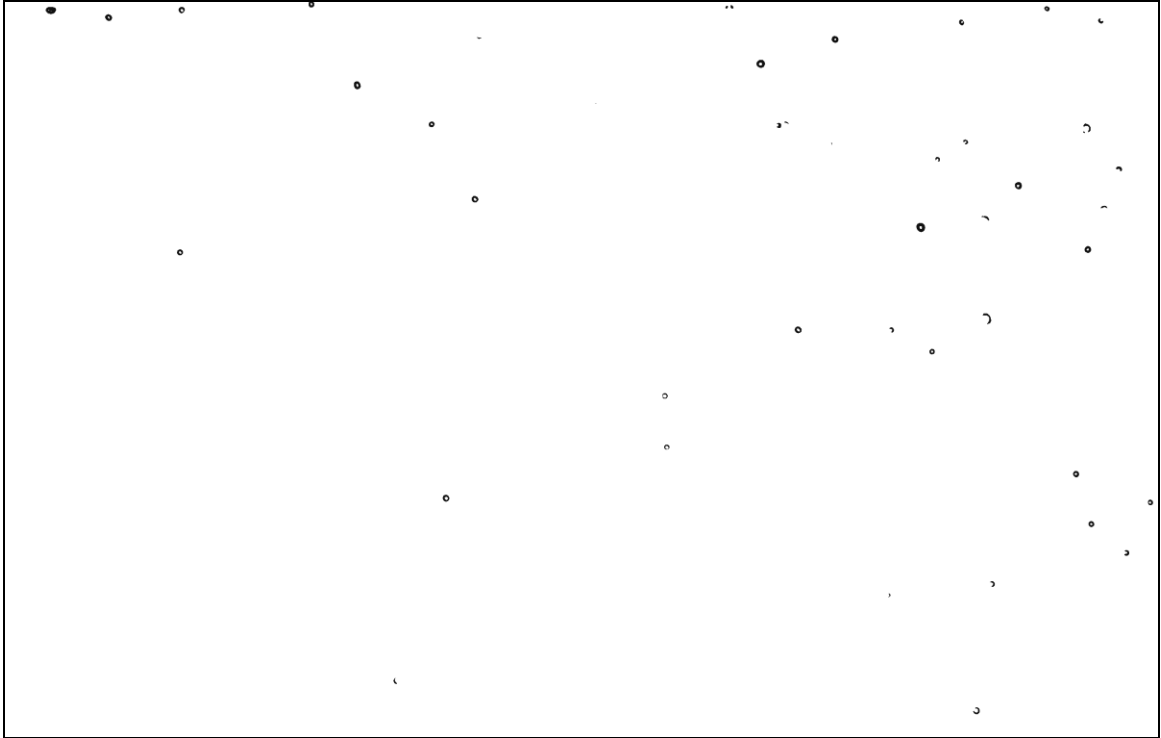


Fig 3.9(g). The filtered image using a threshold level of 100.

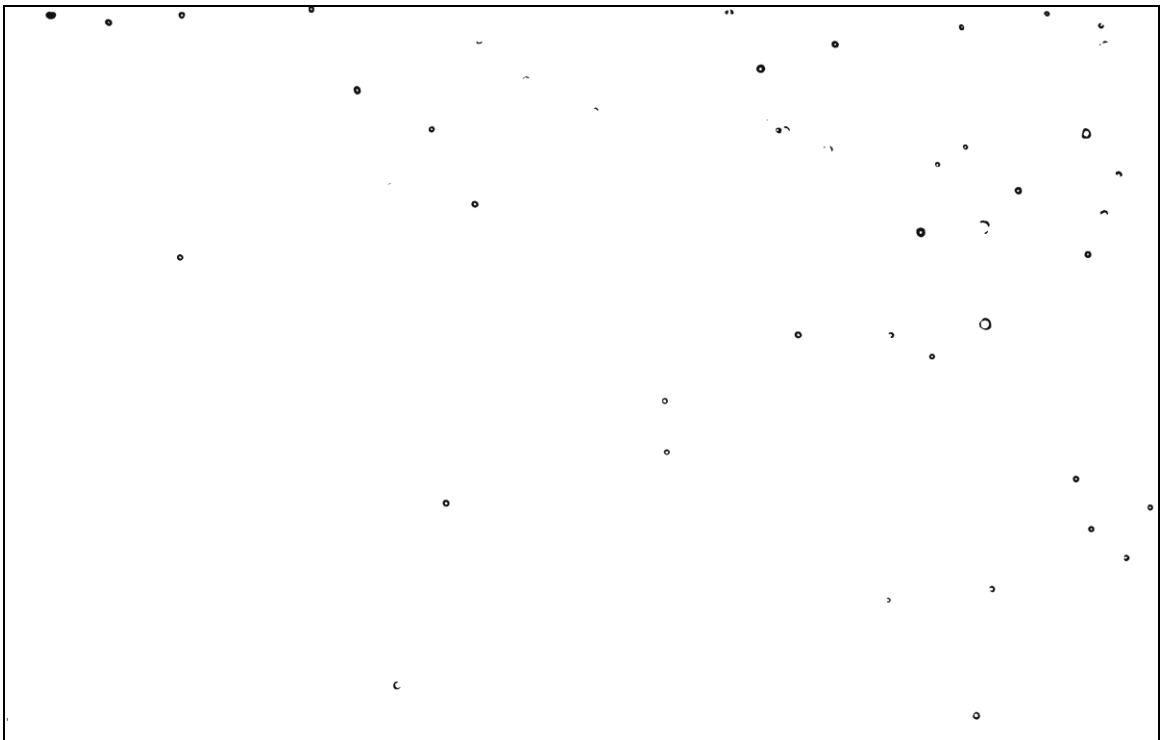


Fig 3.9 (h). The filtered image using a threshold level of 110.

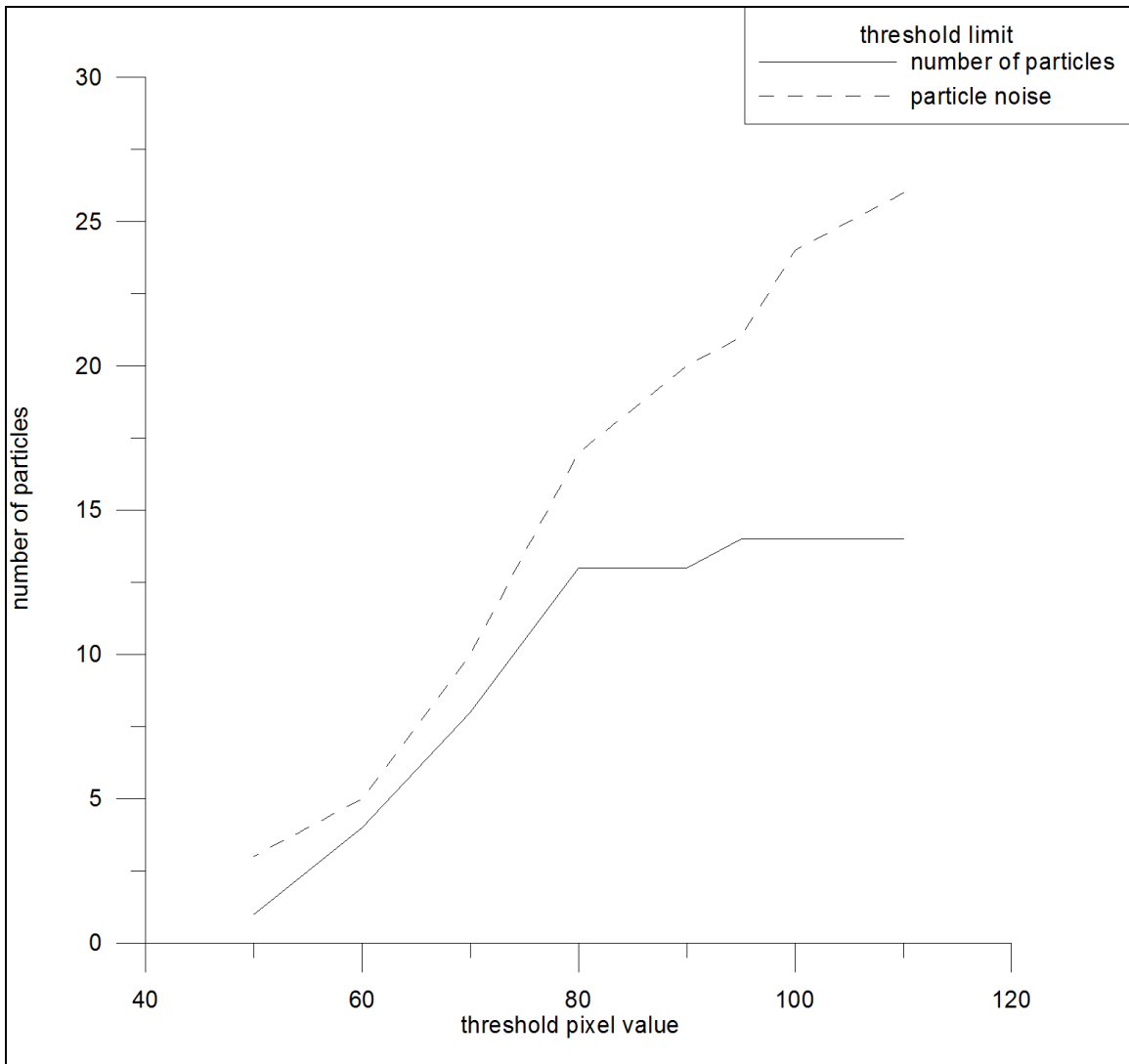


Fig 3.9(i). The number of focused and non focused droplets as function of the threshold value.

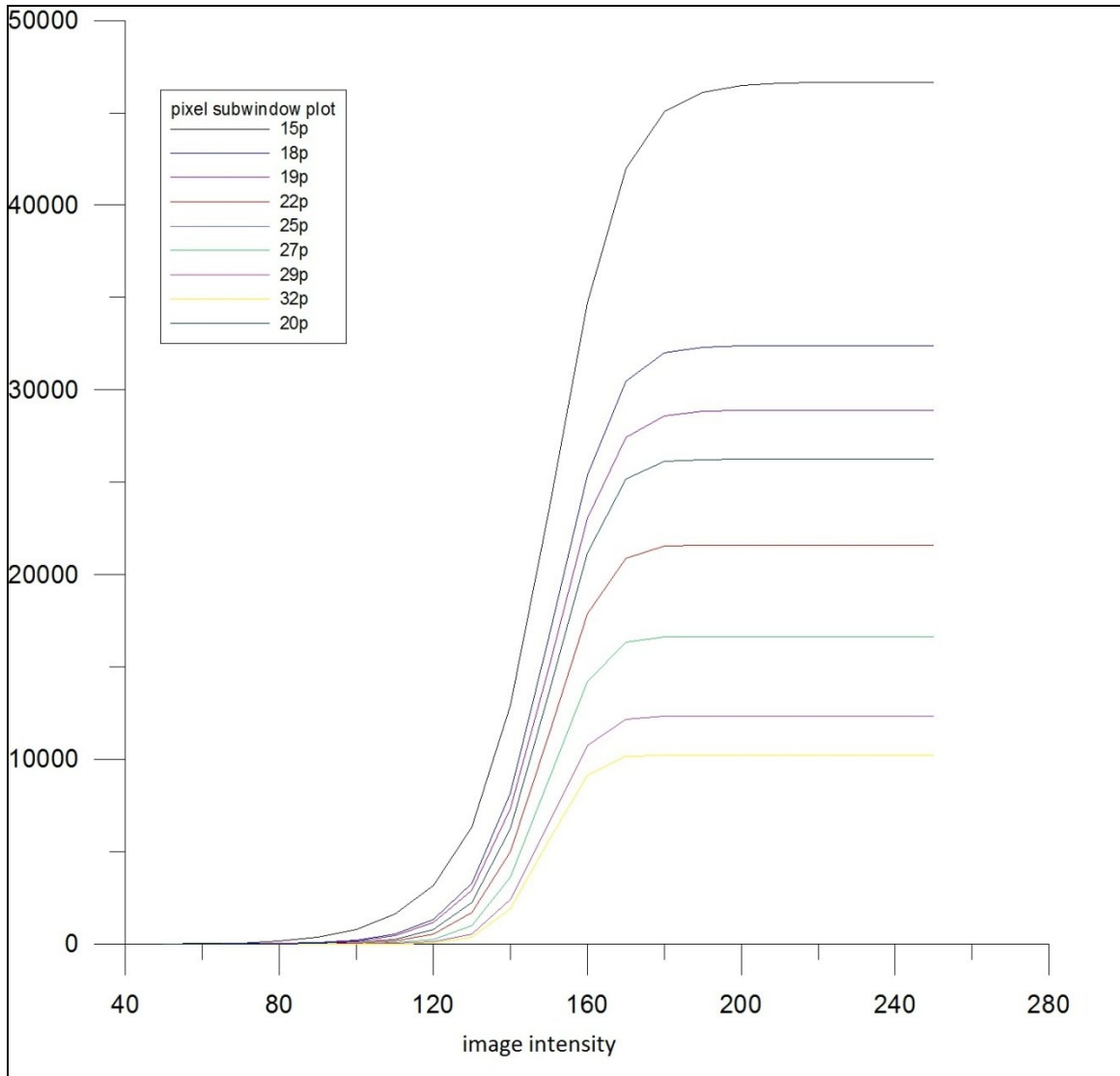


Fig 3.10(a). The number of flagged sub-windows vs. the image (pixel) intensity for different sub-windows sizes.

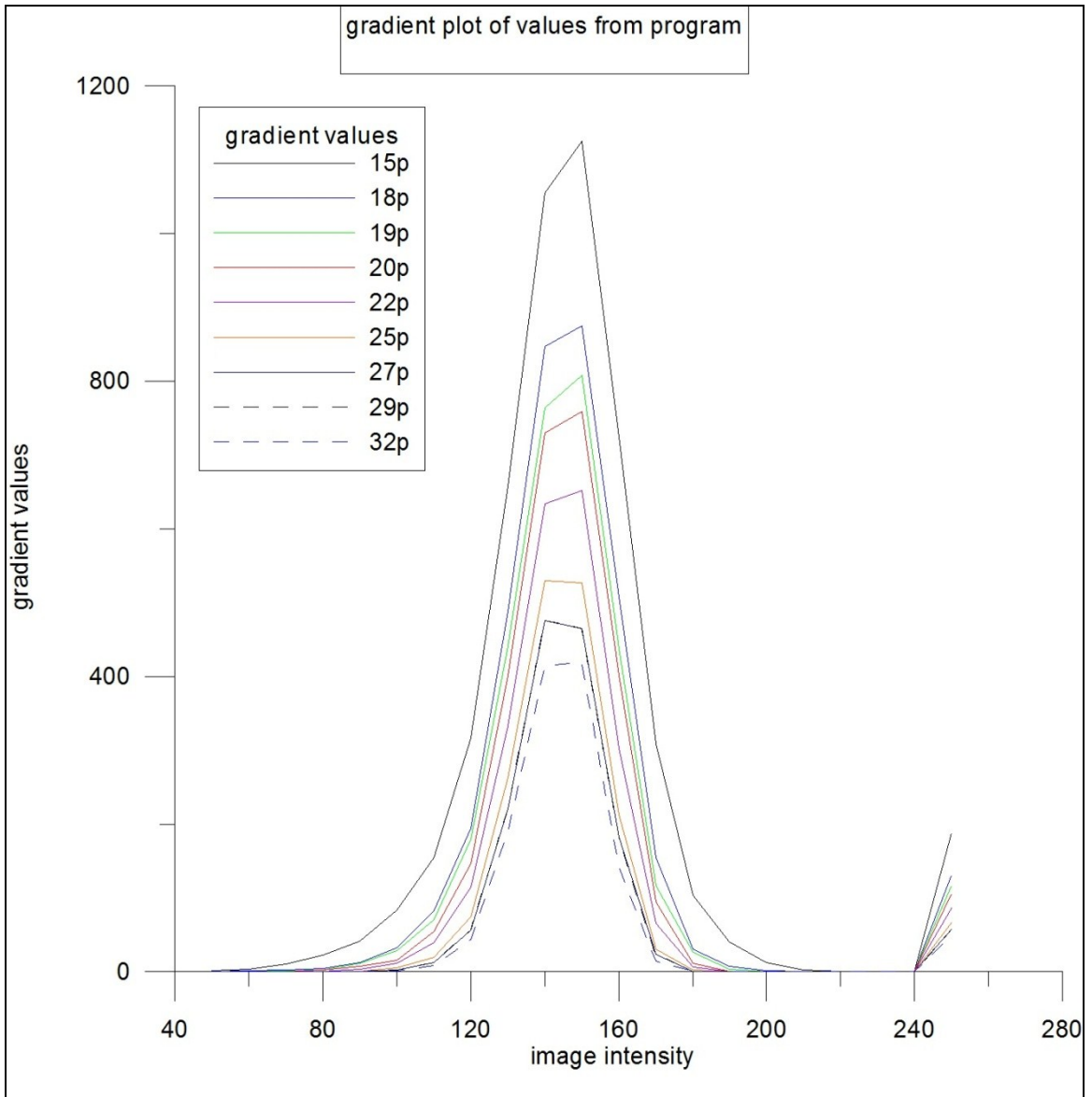


Fig 3.10(b). The gradient of the number of flagged sub-windows vs. the image intensity for various sub-windows sizes.

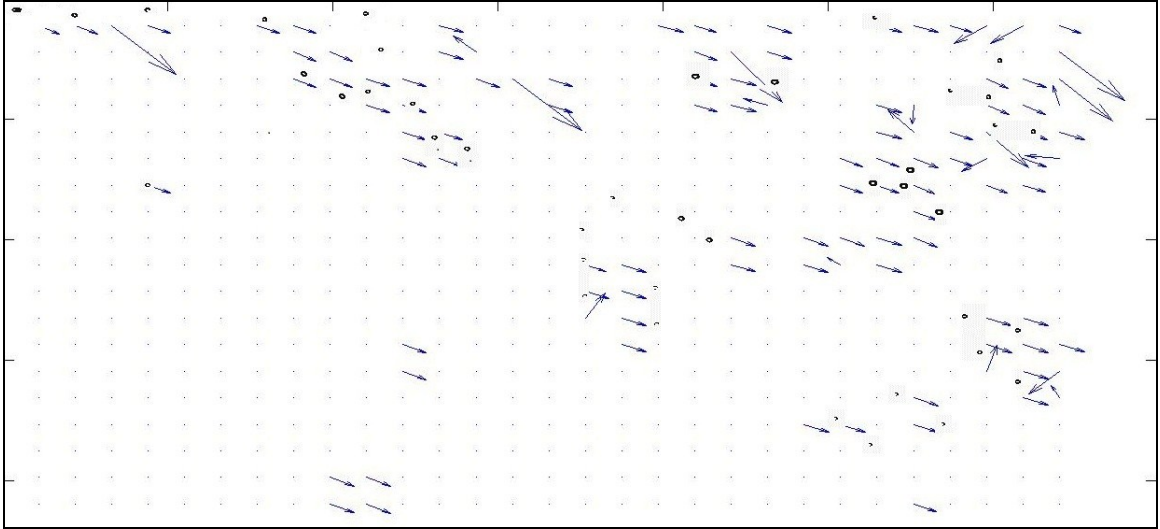


Fig 3.11. Calculated velocity vectors using PIV algorithm.

CHAPTER IV

SUMMARY AND CONCLUSIONS

4.1 Summary

This study involved developing subroutines in MATLAB to apply particle image velocimetry (PIV) to digital holograms of dense spray fields. Holographic PIV techniques are capable of recording three dimensional particle velocity fields. However, to make this measuring technique applicable to sprays one needs to resolve the problems associated with the presence of large number of in-plane (focused) and out-of-plane (unfocused) droplets in the reconstructed two-dimensional images (slides) of the spray field. . The first step was to add numerically the reconstructed slides to make focused droplets darker than the background and the unfocused droplets lighter in final slide (also referred to as master slide). This difference is even amplified using a filtering technique based on thresholding process with different pixel values that can be calculated automatically. This threshold filtering process helped in removing the unfocused droplets from the master slides and made the slides easier to process using PIV. MATPIV (freeware) subroutine was used to correlate the spray holograms taken at two time instances. The present results show that the developed subroutines can be used effectively to apply PIV subroutines to digital holograms of spray fields.

4.2 Conclusion

The major conclusions of present study are as follows:

1. Using the image processing procedure developed in this study the focused and unfocused droplets can be distinguished based on their brightness.
2. The automated selection of the thresholding developed in this study would help the user preparing the reconstructed slides for PIV processing.
3. This method present an easy way of calculating the velocity field of sprays and reducing the complexities involved with present methods of particle tracking velocimetry especially when applied to dense sprays.

4.3 Future Work

The present study shows that PIV techniques can be applied to digital holograms of dense sprays. The following are recommended for a future study:

1. To improve the results of the PIV processing the unfocused droplets need to be removed completely from the reconstructed slides using a more conservative filtering technique.
2. An edge detection method can be introduced to reduce the probability of losing focused droplets during the filtering processes.

3. To calculate the three dimensional velocities an orthogonal view can be introduced in the optical setup. The velocity vectors calculated from applying PIV to both views can then be matched.

REFERENCES

Adrian R., "Multi Point optical measurements of simultaneous vectors in unsteady flow-a review", International journal of heat and fluid flow, 1986, Vol. 7, No. 2 , pp. 127-134.

Barnhart D., Halliwell N., and Coupland J., "Holographic particle image velocimetry: analysis using a conjugate reconstruction geometry", Optics and laser technology 2000, Vol. 32. , pp. 527-533.

Cao L., Gang P., Jeremy J., Scott W., and Hui M., "Hybrid digital holographic imaging system for three dimensional dense particle field measurement", 2008, Applied optics, Vol. 47, No. 25., pp. 4501-4508.

Coupland J., Garner R., and Halliwell N., "Holographic particle image velocimetry and its application in engine development" Journal of physics: conference series, 2006, Vol. 45, pp. 29-37.

Fabry E., "3D holographic PIV with a forward scattering laser sheet and stereoscopic analysis", Experiments in fluids, 1998, Vol. 24, pp. 36-46.

Feldmann O., Mayinger E., and Gebhard P., "Evaluation of pulsed laser holograms of flashing sprays by digital image processing and holographic particle image velocimetry", Nuclear engineering and design, 1998, Vol. 184, pp. 239-252.

Hinsch K.D., "holographic particle image velocimetry", Measurement Science and technology, 2002, Vol.13, pp. r61-r72.

Lobutova E., Resagk C., and Putze T., "Investigation of large scale circulations in room air flows using three dimensional particle tracking velocimetry", 2010, Building and Environment, Vol. 45, No. 7, pp. 1653-1662.

Lee J., Miller B., and Sallam K.A., "Demonstration of Digital Holographic Diagnostics for the Breakup of Liquid Jets Using a Commercial-Grade CCD Sensor," *Atom. Sprays*, 2009, Vol. 19, No. 5, pp. 445-456.

Malek M., Allano D., Coetmellec S., Ozkul C., and Lebrun D., "Digital in-line Holography for three dimensional two components particle tracking velocimetry", *Measurement Science and technology*, 2004, Vol. 15, pp. 699-705.

Pope S., "Turbulent flows", Cambridge University Press, Cambridge, 2000

William D., Poon T., "Digital holography and three-dimensional display: principles and applications (Poon ting chung, Editor), Springer link, New York, chap 4., 2010.

Sheng J., Malkiel E., and Katz J., "Single beam two views holographic particle image velocimetry", *Applied optics*, 2003, Vol. 42, pp. 235-250.

Sheng J., Malkiel E., and Katz J., "Digital holographic microscope for measuring three dimensional particle distributions and motions", *Applied optics*, 2006, Vol. 45, pp. 3893-3901

Sheng J., Malkiel E., and Katz J., "Using digital holographic microscopy for simultaneous measurements of 3D near wall velocity and wall shear stress in a turbulent boundary layer", *Experiments in Fluids*, 2008, Vol. 45, pp. 1023-1035.

Soria J., and Atkinson C., "Towards 3C-3D digital holographic fluid velocity vector field measurement-Topographic digital holographic PIV", *Measurement science and technology*, 2008, Vol. 19, pp. 1-12.

Sveen J., and Cowen E., "An introduction to MatPIV v 1.6.1", eprint series, Dept of Math. University of Oslo, "mechanics and applied mathematics", 2004, No. 2 ISSN 0809-4403.

Stanislas M., Okamoto K., and Kaehler C., "Main results of the Second International PIV Challenge", *Measurement Science and Technology*, 2003, Vol.14, pp. R63-R89.

Trolinger J., Belz R.A., and Farmer W.M., “Holographic techniques for the study of dynamic particle fields”, *Applied optics*, 1969, Vol. 8, No. 5

William D., Poon T., “Digital holography and three-dimensional display: principles and applications (Poon ting chung, Editor), Springer link, New York, chap 4., 2010.

Westerweel J., Stanislas M., Okamoto K., and Kaehler C., “Main results of the second international PIV challenge”, *Experiments in Fluids*, 2005, Vol. 39, No. 2, pp. 170-191.

APPENDIX A

MATLAB SUBROUTINES FOR IMAGE PROCESSING

A.1. Matlab program for hologram reconstruction

```
clc
%clear all
%Hologram Input
disp('Step 1. Read the image file into matrix');
h=imread('left_laser_0004A','TIF');
[Ny Nx Nz]=size(h);
if Nz>1
    h=rgb2gray(h);
end
h0=double(h);
[Ny Nx]=size(h0); %Ny= number of rows Nx= number of column
if Nx>Ny %remove the extra column to make image square
    S=Nx-Ny;
    h0(:,1:S/2)=[];
    h0(:,Ny+1:Nx-S/2)=[];
elseif Nx<Ny %remove the extra rows to make image square
    S=Ny-Nx;
    h0(1:S/2,:)=[];
    h0(Nx+1:Ny-S/2,:)=[];
end
disp('dimensions of the images');

[Ny Nx]=size(h0);
lambda=.532; %the wavelength of laser in micron
dxh=7.8;
dyh=7.8;
M=2; %Enter desired magnification (this will change location of focused image)%
first=50; %first reconstruction distance
last=400; %last reconstruction distance
step=10; %step size for reconstruction images
disp('Step 2. Numerical reconstruction of the images');
```

```

%Method A: constructing the images using matrix instead of FOR loop
A=ones(Ny,Nx);
if(Ny>Nx)
    coef0=diag(1:Ny)*ones(Ny);
else
    coef0=diag(1:Nx)*ones(Nx);
end
coef1=coef0(1:Ny,1:Nx);
coef2=coef0(1:Nx,1:Ny)';
%End of Method A

for D = first: step: last; %Input the range of reconstruction distances in mm must be
between 200mm and 800mm with minimum spacing of 1mm
    disp('Reconstruction in progress.....');
    d=D*1000; %converts to microns%

    dr=230; %distance from source point to CCD in recording phase%
    dr=dr*1000; %converts to microns%
    xrprime=Nx/2; %location of source point in reconstruction phase (usually centered)%
    yrprime=Ny/2; %location of source point in reconstruction phase (usually centered)%
    dprime=d*M; %reconstruction distance%
    drprime=(1/dprime-1/d+1/dr)^(-1); %location of source point in reconstruction phase%
    %c=-i*2*pi*dprime/lambda; %constant%

%Method A: constructing the impulse response using matrix instead of FOR loop
    coff1=((dprime^2)*A+((coef1-(A*Nx/2)).^2)*(dxh^2)+((coef2-
(A*Ny/2)).^2)*(dyh^2)).^0.5;
    g=(1/lambda)*(exp((-i*2*pi/lambda)*coff1))./coff1;
    Er=exp(-i*2*pi/lambda*(A*dprime^2+(coef1-A*xrprime).^2+(coef2-
A*yrprime).^2).^0.5); %Equation for spherical reference beam%
%End of Method A

%Method B: constructing the impulse response using for loop
% for m=1:Ny
%     for n=1:Nx
%         %the impulse response (Eq.3.30 pg53) is calculated for each pixel%
%         coff1=(d^2+((m-Nx/2)^2)*(dxh^2)+((n-Ny/2)^2)*(dyh^2)).^0.5;
%         g(m,n)=(1/lambda)*(exp((-i*2*pi/lambda)*coff1))/coff1;
%     end
% end
%End of Method B
    H0=fftshift(fft2(h0.*Er)); %eq. 3.32
    G=fftshift(fft2(g)); %eq. 3.32
    %imshow(angle(G));
    %figure

```

```

h_Amp=fftshift(iff2(H0.*G)); %eq. 3.32

I=(h_Amp.*conj(h_Amp)); %Multiplies U0 with the complex conjugate of U0% to get
the image intensity
B=max(max(I));
I=I/B;
Imin=min(min(I));
Imax=max(max(I));
I=imadjust(I,[Imin; Imax],[]);
I=(I^(1/6));
imwrite(I,[num2str(D) 'zzmm.JPG']);

%%%%%%%%%%%%%%%%%%%%%%%%%%%%%%%%%%%%%%%%%%%%%%%%%%%%%%%%%%%%%%%%%%%%%%%%
%%%%%%%%%%%%%%%%%%%%%%%%%%%%%%%%%%%%%%%%%%%%%%%%%%%%%%%%%%%%%%%%%%%%%%%%
%clear H_Amp I G g coff1 ;

End

```

A.2. Program for manual threshold

```
%% program for manually thresholding the image%% khuswhant saini
b=imread('1f.tif');%% name of file to threshold

[r,c]= size(b);
for i= 1:r%% checking the value of every pixel
    for j= 1:c
        if (b(i,j)>100)
            b(i,j)=250;%% change value of pixels
        else
            b(i,j)=20;%% change background pixels to lighter values
        end
    end
end

imshow(b);%% display final result
```

A.3. program for threshold using sub-window

```
%% program for threshold image using subwindows%% khushwant saini
bs = [32 32] % size of sub window

% dividing the images
szM = size(M);
nb = szM ./ bs; % number of subwindow in each dimension

C = mat2cell(M, repmat(bs(1),1,nb(1)), repmat(bs(2),1,nb(2)));
% calculating mean for each sub window
C2 = cellfun(@(x) mean(x(:)), C, 'un', 0);
M2 = cell2mat(C2);
M3=floor(M2);
for i=50:10:250%% checking each subwindow for threshold
    m=M3<i;
    a= sum(m(:))

save(['sum',num2str(i),'.mat'],'a');
end
```

A.4. Main routine 'mpiv.m' to run matpiv

```
t = cputime;
D = [];

% transpose of the matrix im#(iy,ix) -> im#(ix,iy)
im1 = double( imr1' );
im2 = double( imr2' );

% check image sizes
nx = size(im1,1);
ny = size(im1,2);
nx2 = size(im2,1);
ny2 = size(im2,2);

if ( nx ~= nx2 ) | ( ny ~= ny2 )
    error('Error: image sizes are different!!!');
end

nx_window = round(nx_window);
ny_window = round(ny_window);

if overlap_x > 0.9 | overlap_y > 0.9
    error('Error: the overlap ratio is too large!!!')
end

disp('Preprocessing finished');

% --- select one of the piv methods for velocity determination

if ( piv_type == 'mqd' ) | ( piv_type == 'MQD' )

    if (abs(i_recur) == 0) | (abs(i_recur) == 1)

        [xi, yi, iu, iv] = piv_mqd( im1, im2, ...
            nx_window, ny_window, ...
            overlap_x, overlap_y, ...
            iu_max, iv_max, ...
            i_recur );

    elseif abs(i_recur) <= 5

        [xi, yi, iu, iv] = piv_mqr( im1, im2, ...
            nx_window, ny_window, ...
            overlap_x, overlap_y, ...
            iu_max, iv_max, ...
```



```

        i_recur );

elseif abs(i_recur) > 5

    error('Error: i_recur is too large !!!');

end

elseif ( piv_type == 'mqc' ) | ( piv_type == 'MQC' )

    [xi, yi, iu, iv, D] = piv_mqd( im1, im2, ...
        nx_window, ny_window, ...
        overlap_x, overlap_y, ...
        iu_max, iv_max, ...
        i_recur );

elseif ( piv_type == 'cor' ) | ( piv_type == 'COR' )

    if (abs(i_recur) == 0) | (abs(i_recur) == 1)

        [xi, yi, iu, iv] = piv_cor( im1, im2, ...
            nx_window, ny_window, ...
            overlap_x, overlap_y, ...
            iu_max, iv_max, ...
            i_recur );

    elseif abs(i_recur) <= 5

        [xi, yi, iu, iv] = piv_crr( im1, im2, ...
            nx_window, ny_window, ...
            overlap_x, overlap_y, ...
            iu_max, iv_max, ...
            i_recur );

    elseif abs(i_recur) > 5

        error('Error: i_recur is too large !!!');

    end

else

    error('Error: invalid piv_type !!! piv_type is case sensitive');

end

% --- dimension for velocity

iu = iu/dt;
iv = iv/dt;

% --- plot image and velocity

```

```

if i_plot == 1
    x = 1:nx;
    y = 1:ny;
    [XV YV] = meshgrid(xi, yi);
    % change image pixel value for plot
    image_max = max(max(im1));
    im = 75*im1/image_max;
    % transpose of the matrix for plotting: (x,y)->(y,x)
    image( x, y, im' );
    colormap(gray)
    hold on
    % transpose of the matrix: (x,y)->(y,x)
    quiver( XV, YV, iu', iv', 'g' );
    hold off
    xlabel('x (pixel)')
    ylabel('y (pixel)')
end

% --- output mean displacement, maximum displacement, elapstime,
%       and number of valid vectors

iu_tmp = reshape(iu, 1, size(iu,1)*size(iu,2));
tmp     = find(~isnan(iu_tmp));
iu_tmp = iu_tmp(tmp);
iv_tmp = reshape(iv, 1, size(iv,1)*size(iv,2));
tmp     = find(~isnan(iv_tmp));
iv_tmp = iv_tmp(tmp);
elapstime = cputime - t;

disp(' ')
disp(' ===== ')
c_tmp = strcat( '> Mean displacement in x and y (pixel) = ', ...
               num2str(nanmean2(abs(iu_tmp)), '%8.4f'), ', ', ...
               num2str(nanmean2(abs(iv_tmp)), '%8.4f') );

disp( c_tmp )
c_tmp = strcat( '> Maximum displacement in x and y (pixel) = ', ...
               num2str(max(max(abs(iu_tmp))), '%8.4f'), ', ', ...
               num2str(max(max(abs(iv_tmp))), '%8.4f') );

disp( c_tmp )
c_tmp = strcat( '> Number of valid vectors versus total vectors = ',
               ...
               num2str(length(tmp), '%8.0f'), ', ', ...
               num2str(size(iv,1)*size(iv,2), '%8.0f') );

disp( c_tmp )
c_tmp = strcat( '> Elapsed time (second) = ',
               num2str(elapstime, '%15.7e') );
disp( c_tmp )
disp(' ===== ')

```

APPENDIX B

VALIDATION OF PIV RESULTS

B.1. Plot of vectors when slides are threshold at different image intensity.

To prove the effectiveness of threshold operation the vectors are calculated by using MATPIV before and after thresholding the slides at different image intensity. Fig B 1.1 shows the vectors calculated from slides without threshold, due to presence of unfocused droplets a lot of vectors are present in image.

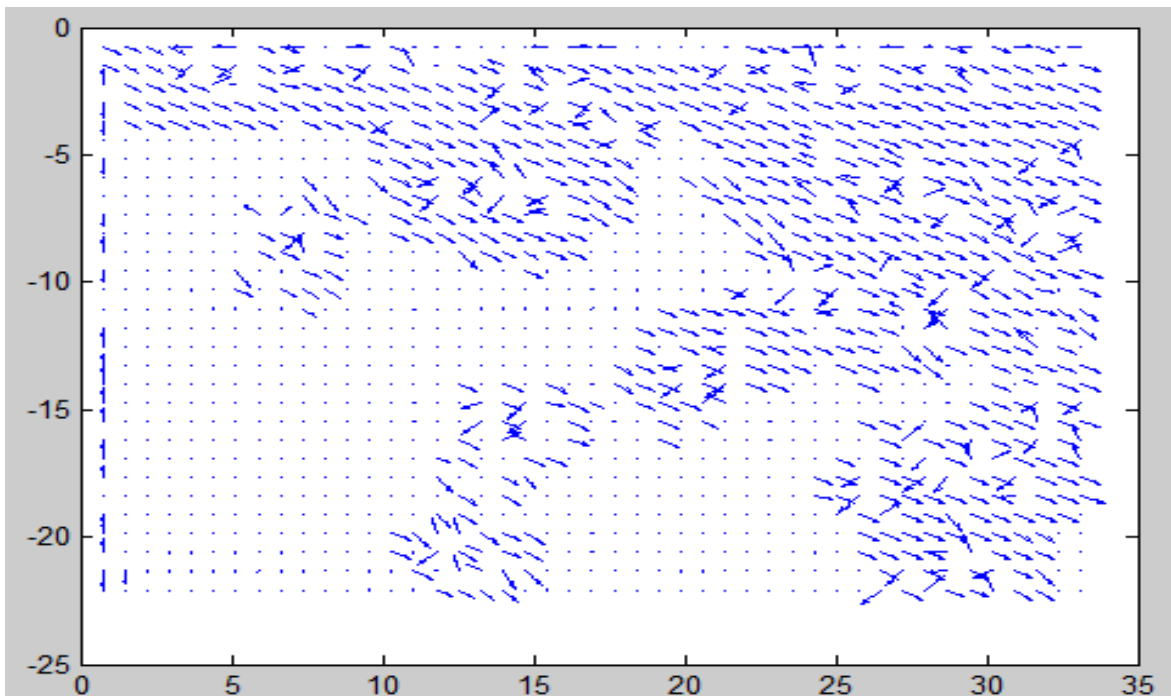


Fig B 1.1. Plot of vectors without threshold

The given plots show the vectors calculated by processing the slides thresholded at different image intensity.

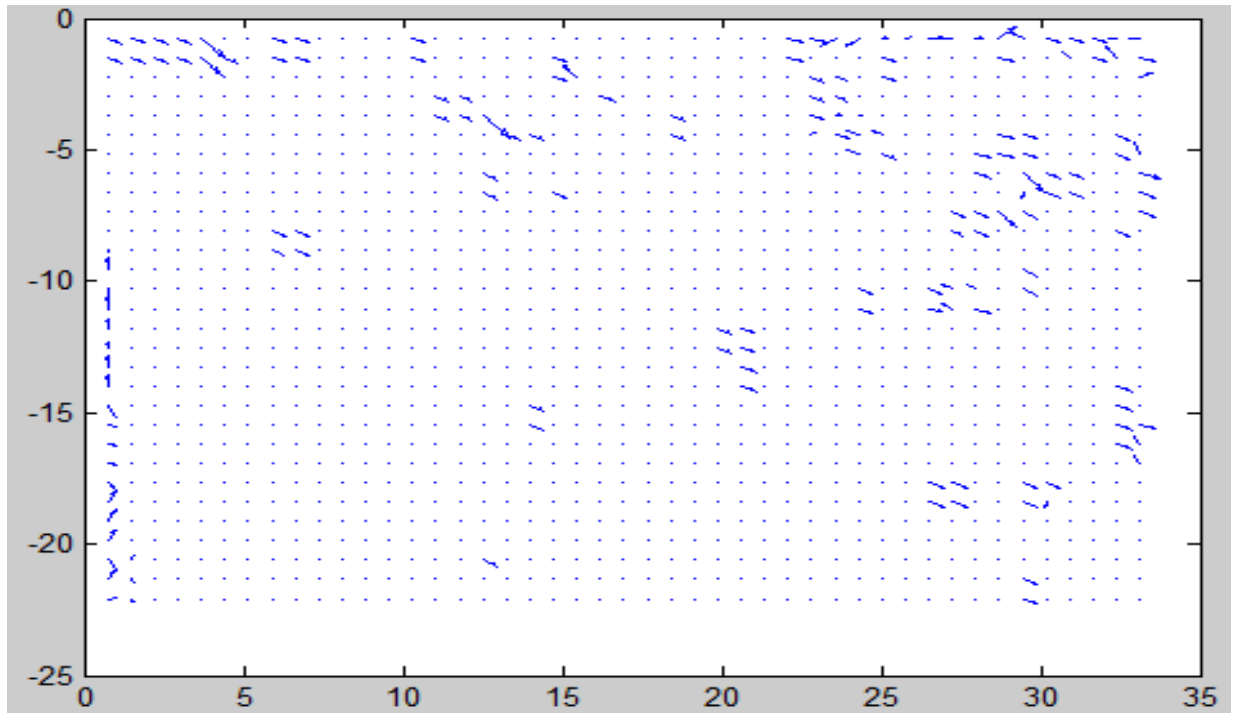


Fig B 1.2. Plot of vectors from slide threshold at 80.

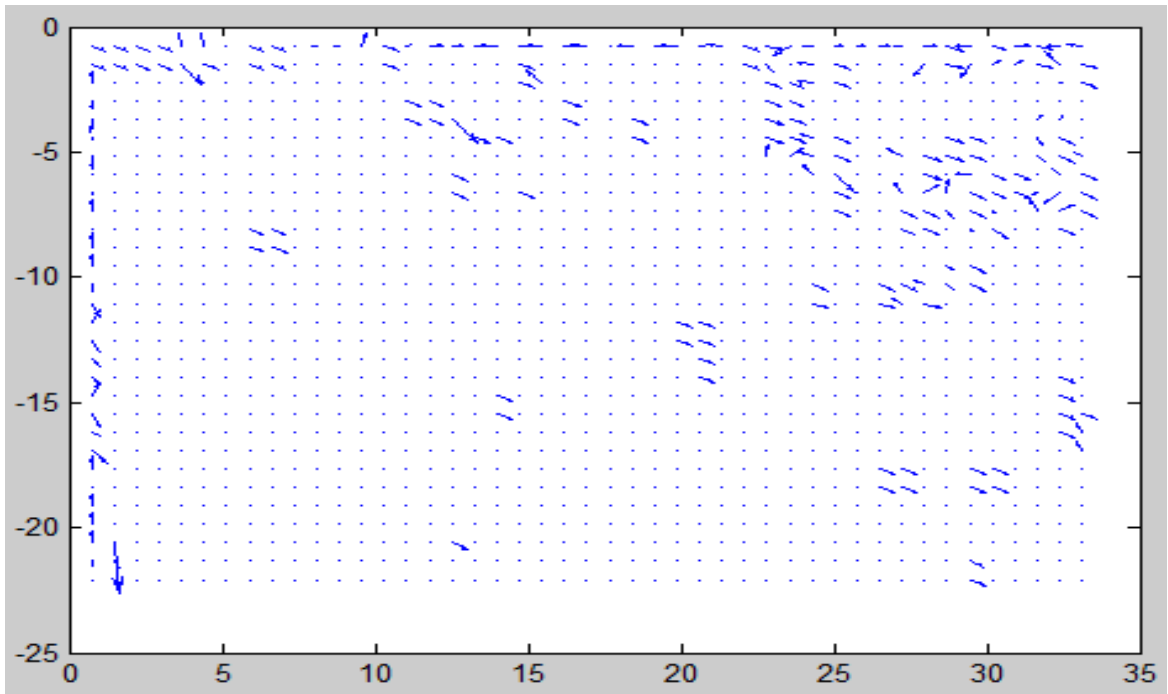


Fig B 1.3. Plot of vectors from slide threshold at 110.

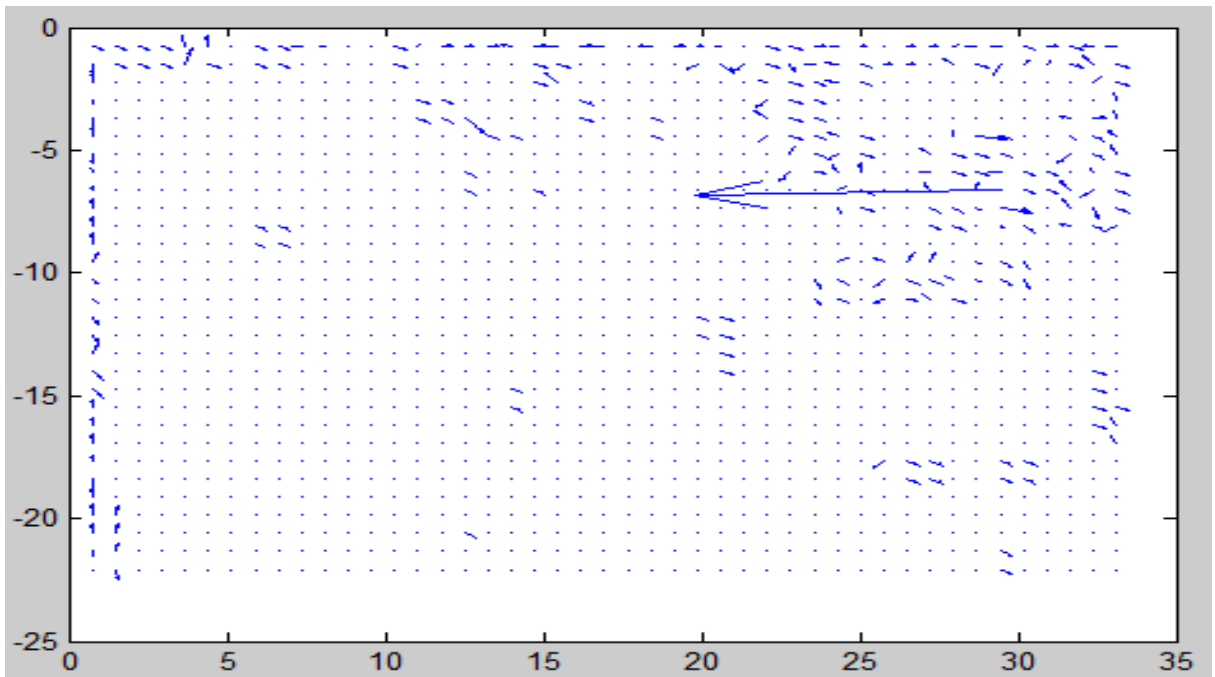


Fig B 1.4. Plot of vectors from slide threshold at 120.

As we can see from the vector plots if we increase the threshold level a lot of error vectors comes into result, while reducing the threshold level also effect the actual velocity. To make a comparison of error, deviation from actual velocity is calculated by comparing the mean velocity from every plot with actual mean velocity. Actual velocity is calculated by measuring the shift of droplets in pixel manually. Table B1 shows the error in (%) calculated at different threshold level.

Table B1. Error in velocity

Threhold level	Total vectors	bad vectors	Mean velocity	Actual velocity	Error(%)
80	137	32	67	64.1	-4.5
100	219	35	64.6	64.1	-2.34
110	247	54	61.4	64.1	4.21
120	283	90	34.17	64.1	46.7

VITA

Khushwant Saini

Candidate for the Degree of

Master of Science

Thesis: VELOCITY MEASUREMENTS USING HOLOGRAPHIC PARTICLE
IMAGE VELOCIMETRY

Major Field: Mechanical and Aerospace engineering

Biographical: Khushwant Saini is the son of B.D. Saini and Usha Saini and a resident of
Ratlam Madhya Pradesh, India

Education: Received BE(mechanical engineering) from university of Rajiv
Gandhi Technical University, Bhopal in 2004 pursuing the requirements
for the master of science in Mechanical and aerospace engineering at
Oklahoma State University, Stillwater, Oklahoma.

Experience: Employed by Oklahoma State university as a teaching assistant for
computational methods in VBA, thermodynamics and machine shop
from August 2009 till December 2010 and as a Research assistant from
May2009 to July 2009.

Professional Memberships:

The American Society of Mechanical Engineering.

The American Institute of Aeronautics and Astronautics.

Society Of Automotive Engineers.

Name: Khushwant Saini

Date of Degree: December, 2010

Institution: Oklahoma State University

Location: Stillwater, Oklahoma

Title of Study: APPLYING HOLOGRAPHIC PARTICLE IMAGE VELOCIMETRY TO
SPRAYS

Pages in Study: 61

Candidate for the Degree of Master of Science

Major Field: Mechanical and Aerospace engineering

Scope and Method of Study: Measuring the velocity field of dispersed flows is of major importance in many applications, such as sprays and particle-laden jets. The present study involved extension of present holographic PIV method to spray fields. The present optical setup is based on inline digital holographic microscopy. Double-pulsed holograms were recorded and reconstructed to yield many two-dimensional slices (planes) of the flow field at two time instances. A large number of focused and unfocused drops appeared in each slice resulting in a lot of noise. Thus it was required to develop new image processing subroutines which could bypass the noise and consider only the focused droplets present in each plane while rejecting the shadow of non focused droplets not present in plane. Matlab routines were developed to filter the slides and to reduce the noise level in the reconstructed images from hologram before applying PIV algorithms to them.

Findings and Conclusions: Developed image processing procedure was successfully applied to reduce the noise in the reconstructed hologram slides. Focused and non-focused particles are distinguished by using a program, which was based on difference in brightness value of the particles in the image. Manual and automated threshold programs were developed to help user in deciding the threshold level for removing the non-focused droplets. Sensitivity of noise to threshold intensity was investigated with the help of threshold program and results were compared. Validated PIV routines were used to process the reconstructed slides. Two dimensional velocities for three dimensional spray fields were successfully calculated. Results calculated from PIV routines were compared with actual mean velocity of droplets from image. The proposed method present an easy way of calculating the velocity field of sprays and helped to reduce the complexities involved with present methods of Particle Tracking Velocimetry especially when applied to dense sprays.

ADVISER'S APPROVAL: Khaled A. Sallam
